

FLOATING INSTALLATION OF WINDTURBINE TOWERS

A CONCEPTUAL DESIGN STUDY

J.Termorshuizen

FLOATING INSTALLATION OF WIND TURBINE TOWERS

A CONCEPTUAL DESIGN STUDY

FLOATING INSTALLATION OF WIND TURBINE TOWERS

A CONCEPTUAL DESIGN STUDY

Master thesis

to obtain the degree of Master of Science
at the Delft University of Technology,
to be defended publicly on 10/05/2019

by

Jelmar TERMORSHUIZEN

Faculty of Mechanical, Maritime and Materials Engineering,
TU Delft, Delft, The Netherlands.

Thesis committee:

Dr. ir. P. R. Wellens,	TU Delft, chairman
Dr. ir. P. Naaijen,	TU Delft, daily supervisor
Ir. M. van der Eijk,	TU Delft
Dr. ir. X. Jiang,	TU Delft
Ir. J. Koppenol,	Temporary Works Design



An electronic version of this thesis is available at
<http://repository.tudelft.nl/>.

CONTENTS

List of Figures	vii
List of Tables	xi
List of symbols	xiii
Summary	xvii
Preface	xix
1 Introduction	1
1.1 Introduction To Offshore Wind	2
1.1.1 Developing Markets	2
1.1.2 Offshore Wind Farms	2
1.1.3 Offshore Wind Turbines	3
1.2 Turbine Installation	6
1.2.1 Installation Procedure	6
1.2.2 Turbine Installation Vessels (TIVs)	6
1.2.3 Proposed Future Of The Turbine Installation Vessel	8
1.3 Load Control During Offshore Operations	9
1.3.1 Passive Systems	10
1.3.2 Active Systems	11
1.4 Offshore Wind; The Expectations	12
2 Research Objective	13
2.1 Research Objective	14
2.2 Scope And Aim	14
2.3 Thesis Outline	15
3 Functional Design	17
3.1 Design Strategy	18
3.1.1 Engineering Models Of Product Design	18
3.2 Problem Statement	19
3.2.1 Sub-Problems	19
3.3 Design Requirements And Criteria	20
3.4 Sub-Solutions	21
3.5 Concepts	22
3.5.1 Multi-Criteria Analysis	25
3.6 Concept Performance.	27

4	Vessel-Tower Model	29
4.1	Reference Frames	30
4.2	Vessel Model	31
4.2.1	Vessel Conventions	31
4.2.2	Simulation Vessel	32
4.2.3	Vessel Motions	32
4.2.4	Response In Waves.	34
4.2.5	Response Of Crane Tip.	34
4.3	Tower Model	35
4.3.1	2D Model	36
4.3.2	Lagrangian Mechanics	38
4.3.3	Deriving The Equations Of Motion.	39
4.3.4	Eigenmodes	40
4.3.5	Motion Compensation System.	41
4.3.6	Transfer Function Derivation	43
4.3.7	Validation Of The Transfer Function	45
4.3.8	Coupling Of Tower And Vessel Response	47
4.4	Optimization	49
4.5	Orcaflex.	54
4.5.1	Model	54
4.5.2	Validating The Transfer Functions	57
4.5.3	Time Domain Simulation	61
4.5.4	Comparing The Different Simulation Methods.	68
4.5.5	Conclusions And Discussion Time Domain Simulations.	68
5	Conclusion and Recommendations	71
5.1	Conclusions.	72
5.1.1	Sub-Objectives.	72
5.1.2	Main Objective.	73
5.2	Recommendations	73
	Bibliography	75
A	Concept Evaluation	77
A.1	Concept Re-evaluation	78
A.1.1	Optimal Configurations	79
A.2	Conclusions.	83

LIST OF FIGURES

1.1	Market forecast: 16% annual growth rate of the globally installed capacity forecasted by BloombergNEF	2
1.2	Offshore wind farms located in the North Sea.	3
1.3	Graphical representation of the different components of an offshore wind turbine.	4
1.4	Offshore wind turbine support structures. From left to right: gravity based, monopile, caisson, multi-pile, multi-caisson and jacket	5
1.5	Increase of offshore wind turbine dimensions over time (turbine data from UK, NL, DE and DK).	5
1.6	Installation sequence jack-up vessel.	6
1.7	Two generations of jack-up vessels; MPI Resolution [l], Seajacks Scylla [r] .	7
1.8	Dedicated turbine installation concepts; Huisman [l], IHC Vuyk [m], Ulstein [r]	7
1.9	Orion (DEME) [l], Bokalift 1 (Boskalis) [r]	8
1.10	Guiding a lifted object during installation jobs; human guidance [l], guiding funnels/holes [m], guiding piles [r]	10
1.11	Cranemaster used for lifting a transition piece.	10
1.12	Usage of taglines during lifting; manual control [l], attached to lifting gear [m], automatically controlled system [r]	11
1.13	Motion compensated pile gripper.	11
1.14	Current generation of motion compensated cranes, MacGregor [l], Ulstein [r].	12
2.1	Installation cycle	14
2.2	Installation phases. From left to right: lift-off from sea fastening, move-out to TP, positioning above TP, touch-down on TP	15
3.1	Model flow	18
3.2	Morphological chart.	22
3.3	Concept 1: using cables to 'steer' the tower during lifting.	23
3.4	Concept 2: grabbing the tower around C.o.G..	23
3.5	Concept 3: combining two existing motion compensation systems.	24
3.6	Concept 4: motion compensated crane.	24
3.7	Concept 5: combining two motion compensated grippers.	25
4.1	Reference frame.	30
4.2	Definition of the vessel motions.	31
4.3	Vessel similar to the simulation vessel.	32

4.4	Graphical representation of the real parts of the surge, sway and heave RAOs at the crane tip position for an incoming wave direction of 180 degrees.	35
4.5	Lowering of the tower to the moment just before touchdown [r].	36
4.6	Graphical representation of the double pendulum model.	38
4.7	Eigenperiods and eigenfrequencies of the system.	40
4.8	Double pendulum model (including spring-damper system)	42
4.9	Simple pendulum on cart.	46
4.10	Comparing the transfer functions of the simple pendulum on a cart with the double pendulum ($l_T \ll 1$) [l] and the double pendulum ($l_T = 100m$) [r]	47
4.11	Transfer function relating the horizontal top displacement of the tower to the sea surface elevation for a varying position of the motion compensation system [l], $k = 1000kN/m$ and $c = 100kNs/m$	48
4.12	Transfer function relating the horizontal bottom displacement of the tower to the sea surface elevation for a varying position of the motion compensation system, $k = 1000kN/m$ and $c = 100kNs/m$	49
4.13	Influence of lifting and lowering the tower on the optimized value of the cost function and the corresponding values of a , k and c	51
4.14	Values of the costfunction of the 6 MW tower for various a and k , $c = 53kNs/m$ and $l_{wr} = 40m$	52
4.15	Values of the costfunction of the 6 MW tower for various a and k , $c = 53kNs/m$ and $l_{wr} = 25m$	53
4.16	Orcaflex model.	54
4.17	Comparison of the TFs x_{top}/ζ obtained using multiple simulation methods (6 MW tower).	58
4.18	Comparison of the TFs x_{bot}/ζ obtained using multiple simulation methods (6 MW tower).	58
4.19	Comparison of the TFs x_{top}/ζ obtained using multiple simulation methods (8 MW tower).	59
4.20	Comparison of the TFs x_{bot}/ζ obtained using multiple simulation methods (8 MW tower).	59
4.21	Orcaflex time domain configurations: free hanging tower [l], compensated tower [r].	61
4.22	Translations of the crane tip.	62
4.23	Free translations of the top of the 6MW tower.	63
4.24	Free translations of the bottom of the 6MW tower.	63
4.25	Free translations of the top of the 8MW tower.	64
4.26	Free translations of the bottom of the 8MW tower.	64
4.27	Translations of the top of the 6MW tower for $a = 0.69$, $k = 291kN/m$, $c = 53kNs/m$. Motion compensation applied in x- and y-direction.	65
4.28	Translations of the bottom of the 6MW tower for $a = 0.69$, $k = 291kN/m$, $c = 53kNs/m$. Motion compensation applied in x- and y-direction.	66
4.29	Translations of the top of the 8MW tower for $a = 0.81$, $k = 319kN/m$, $c = 60kNs/m$. Motion compensation applied in x- and y-direction.	67

4.30	Translations of the bottom of the 8MW tower for $a = 0.81$, $k = 319kN/m$, $c = 60kNs/m$. Motion compensation applied in x- and y-direction.	67
A.1	Optimal configuration for the 6 MW tower [l], Optimal configuration for the 8 MW tower [r]	80
A.2	Schematical representation of the Tugger winch concept	81
A.3	Schematical representation of the MCPG concept	83

LIST OF TABLES

1.1	Comparing the different turbine installation vessels.	9
3.1	Multi-criteria analysis of the different concepts.	26
3.2	Scaling factors used to score the concepts.	26
4.1	Tower dimensions	36
4.2	Optimal compensating configurations for both towers.	52
4.3	Standard deviations of the response of the 6 MW tower for the different frequency domain methods.	60
4.4	Standard deviations of the response of the 8 MW tower for the different frequency domain methods.	60
4.5	Comparing the standard deviations of the response of the 6 MW tower calculated using the different methods.	68
4.6	Comparing the standard deviations of the response of the 8 MW tower calculated using the different methods.	68
A.1	Multi-criteria analysis of the different concepts.	78
A.2	Scaling factors used to score the concepts.	79
A.3	Initial and updated ratings of the Tugger winch concept.	80
A.4	Initial and updated ratings of the MCPG concept.	82
A.5	Multi-criteria analysis of the different concepts.	84

LIST OF SYMBOLS

Acronyms

C.o.G.	center of gravity
CT	crane tip
DNV	Det Norske Veritas
EoM	equation of motion
FD	frequency domain
GW	giga watt
HLV	heavy lift vessel
kW	kilo watt
MCA	multi-criteria analysis
MCPG	motion compensated pile gripper
MDOF	multi degree of freedom
MPM	most probable maximum
MW	mega watt
RAO	response amplitude operator
RMS	root mean square
SA	spectral response analysis
SWL	still water level
TIV	turbine installation vessel
TP	transition piece
TWD	Temporary Works Design
WTG	wind turbine generator

Greek Symbols

ω	wave frequency
----------	----------------

Hz

ϕ, θ, ψ	roll, pitch and yaw motion vessel	deg/m
θ_0	pendulum angle (general)	deg
θ_1	angle between crane wire and vertical	deg
θ_2	angle between tower and vertical	deg
ζ	sea surface elevation	m
ζ^*	effective sea surface elevation	m
Roman Symbols		
\dot{q}_j	generalized velocity	m/s
$\bar{x}_{i/3}$	significant response amplitude	m
A	added mass matrix	kg
a	parameter to indicate the position of the motion compensation system along the tower height	–
a_v	added mass	kg
A_{wr}	cross sectional area of crane wire	mm^2
B	damping matrix	Ns
b_v	damping coefficient	kg/s
C	stiffness matrix	N/m
c	virtual damping motion compensation system	kNs/m
$C(a, k, c)$	cost function	m
c_v	restoring spring coefficient	N/m
CT_{CoG}	position of crane tip w.r.t. the vessel C.o.G.	
D	Rayleigh dissipation function	N/s
E	Young's modulus	N/mm^2
F_d	diffraction force	N
F_e	external force	N
F_{FK}	Froude-Krylov force	N
F_h	hydromechanic force	N
g	gravitational acceleration	m/s^2

G_T	tower C.o.G. wrt fixed earth	
G_v	vessel C.o.G. wrt fixed earth	
H_{fi}	complex force transfer function	N/m
H_s	significant wave height	m
H_{xi}	complex transfer function relating the vessel motions to the sea surface elevation	–
I	tower moment of inertia	$tonm^2$
J	moment of inertia	kgm^2
K	stiffness matrix double pendulum	N/m
k	virtual stiffness motion compensation system	kN/m
k_{wr}	stiffness crane wire	N/m
L	Lagrangian	N/m
L	length simple pendulum rod	m
l_{CoG}	distance between top of the tower and tower C.o.G.	m
l_T	tower length	m
l_{wr}	length of crane wire	m
M	mass matrix	kg
m	mass	kg
m_0	zero order spectral moment	m^2
M_e	external moment	Nm
m_T	tower mass	ton
$P(t)$	position vector	m
q_j	generalized displacement	m
S_{wave}	wave spectrum	m^2s
T	kinetic energy	Nm
T_p	peak period	s
V	potential energy	Nm
v	velocity (general)	v

x, y, z	surge, sway and heave motion vessel	m
X_i	vector containing the vessel translations and rotations	var
x_{bot}	displacement of the tower bottom in x-direction	m
$x_{C.o.G.}$	x coordinate of C.o.G. tower used for the Lagrange method	m
X_{ct}	vector containing the crane tip translations	m
x_{ct}	crane tip translation in x-direction	m
x_s	spring elongation	m
x_{top}	displacement of the tower top in x-direction	m
y_{bot}	displacement of the tower bottom in y-direction	m
y_{ct}	crane tip translation in y-direction	m
y_{top}	displacement of the tower top in y-direction	m
Z	sea surface elevation	m
z_{bot}	displacement of the tower bottom in z-direction	m
$z_{C.o.G.}$	z coordinate of C.o.G. tower used for the Lagrange method	m
z_{ct}	crane tip translation in z-direction	m
z_{top}	displacement of the tower top in z-direction	m

SUMMARY

The demand for renewable energy is growing, due to a growing awareness among people concerning the effect of fossil fuels on the environment. Governments have signed climate agreements and are obliged to decrease their level of CO_2 emission. This change in attitude regarding the environment led to an upcoming market for renewables. A significant part of the demand for renewable energy is covered by the wind industry, both on- and offshore. Especially the offshore wind market holds huge potential, due to stable wind conditions and growth opportunities. A side effect of the evolving industry is that turbines are increasing in size and are being installed in deeper water depths. It is expected that the methods of installation, currently used in the offshore wind market, will no longer be capable of installing the new generation turbines. Therefore, research must be conducted into new installation methods.

In this thesis installation of wind turbine towers using a heavy lift vessel is opted as an interesting alternative to the current installation methods. However, the concept of floating installation brings both new challenges and opportunities. One of these challenges is how to deal with the vessel motions affecting the installation process.

This report presents a conceptual design study, identifying the steps to be taken during floating installation and introducing concepts to control the tower motions at the moment just before touchdown of the tower on the transition piece. After a first selection, based on requirements and criteria, two concepts are selected for a detailed examination.

To examine the viability of the proposed solutions, research is conducted in the response of the wind turbine tower in the crane as a result of environmental disturbances. The study in this report focuses only on wave disturbances, since these are expected to be the governing factor for the tower response. To begin with, a frequency domain analysis is conducted giving insight in the response behavior of the tower. Changing the position, stiffness and damping of the compensating system, one can alter the system's eigen frequencies and therefore the magnitude of response. Using frequency domain analysis, a parametric optimization study is conducted to find the optimal parameters for the compensating system in order to minimize the tower response. Since, analysis of a system in the frequency domain requires a system to be linear, a time domain simulation is performed to check the effect of any non-linearity's on the response behavior of the tower.

The results of the model show that a significant response of the horizontal tower motions can be accomplished using a generalized model of tower and motion compensation system. However, more research must be conducted to meet the design requirements.

PREFACE

This thesis is submitted to obtain the Master of Science degree at the Delft University of Technology. To obtain this degree, research is conducted into the possibility of installing offshore wind turbine towers using a floating installation vessel. Although the writing of a Master of Science thesis is almost inevitably paired with ups- and downs, it has been a real pleasure being able to contribute to the development of the offshore wind industry.

During the writing of this thesis I've known the support of many, and it would not have been possible to write this thesis without the support of those people.

During the majority of this research Dr. Ir. Peter Naaijen has provided me with guidance and support. Due to unforeseen circumstances and to my great regret, Peter had to (temporarily) abandon his role as supervisor. Nonetheless, Peter taught me a great deal and has significantly contributed to the end result of this research.

I would like to thank Dr. Ir. Peter Wellens and Ir. Martin van der Eijk for their flexibility and in providing last minute guidance during the final stages of this research.

The continues support of my supervisors at TWD, Jim and Jelmer, helped me enormously to find the guidance and structure required to finish this research. Jim helped me improve, and believe in, my technical abilities and provided me the final baggage required to become an engineer. Jelmer helped me to be critical, improve my efficiency and provided me with most valuable practical insights.

Finally, I would like to thank my family, roommates, friends and especially my girlfriend, Myrthe, for their support and believe in me during the last year.

*Jelmar Termorshuizen
Delft, April 2019*

1

INTRODUCTION

The wind, as all sources of renewable energy, has been a present force since the beginning of time. History learns that our ancestors already, successfully, tried to harvest the power of the wind for centuries and centuries. Until in early Egypt the first windmill was invented, the power of the wind was primarily used to propel ships. From that point on, the windmill has mainly been used to pump water from A to B. Centuries later, in 1887, the ancient machine acquired a new purpose: generation of electricity. However, in the fossil-fuel based economy the interest in large scale electricity generation was scarce.

Nowadays, humanity finds itself in a time where the use of fossil fuels is falling into disrepute; people are getting more aware of the way in which their lifestyle impacts the environment. Climate agreements are set and a growing interest in the preservation of the environment is spreading over the earth. This change in attitude has resulted in a continuously growing demand for renewable energy.

1.1. INTRODUCTION TO OFFSHORE WIND

A significant part of this demand is covered by wind generated energy, both on- and offshore. Especially the offshore wind market holds huge potential, due to stable wind conditions and the almost unlimited growth possibilities. This chapter provides a brief introduction to the offshore wind industry.

1.1.1. DEVELOPING MARKETS

In the year 1991 the construction of the Vindeby farm, world's first ever offshore wind farm, was completed off the coast of Denmark. Due to high levelized costs of energy and the uncertain market prospects the offshore wind industry faced a slow start. Northern European countries recognized the potential of offshore wind power and continued investing in the building of wind farms. At the end of 2017, the total installed offshore wind capacity in Europe was 15.78 GW where the globally installed capacity totaled 17.6 GW [BloombergNEF, 2017]. According to WindEurope, the former European Wind Energy Association, Europe's total installed offshore wind capacity will reach 25 GW by 2020 [Intelligence, 2018]. In January 2018 [BloombergNEF, 2017] forecasted the global offshore wind market to grow by 16 % each year up till 2030 (see Fig. 1.1), resulting in a six-fold multiplication of the totally installed offshore wind capacity with respect to end 2017.

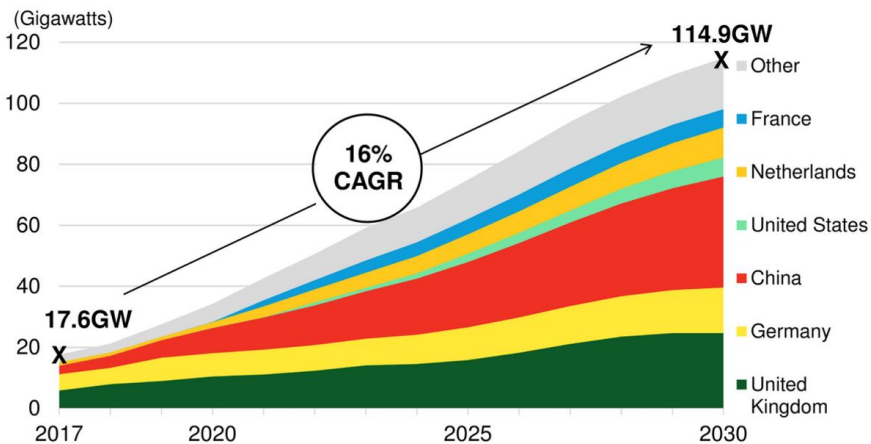


Figure 1.1: Market forecast: 16% annual growth rate of the globally installed capacity forecasted by BloombergNEF

1.1.2. OFFSHORE WIND FARMS

An offshore wind farm consists of a number of wind turbines built in close proximity of each other with the goal to generate energy. The first wind farms have been built on near shore locations with limited water depths. As more and more wind farms are being built in European waters, Europe is running out of 'easy' locations to build offshore wind farms. As a result, the industry is moving to locations further offshore and/or with deeper water depths. An overview of windfarms currently installed in the North Sea is given in Figure 1.2. As mentioned in Section 1.1.1 the majority of the global offshore wind

capacity has been installed in Europe. Although non-European countries like Taiwan, China and the United States are gaining foothold in the offshore wind industry, their installed capacity is still largely outnumbered by the European farms.

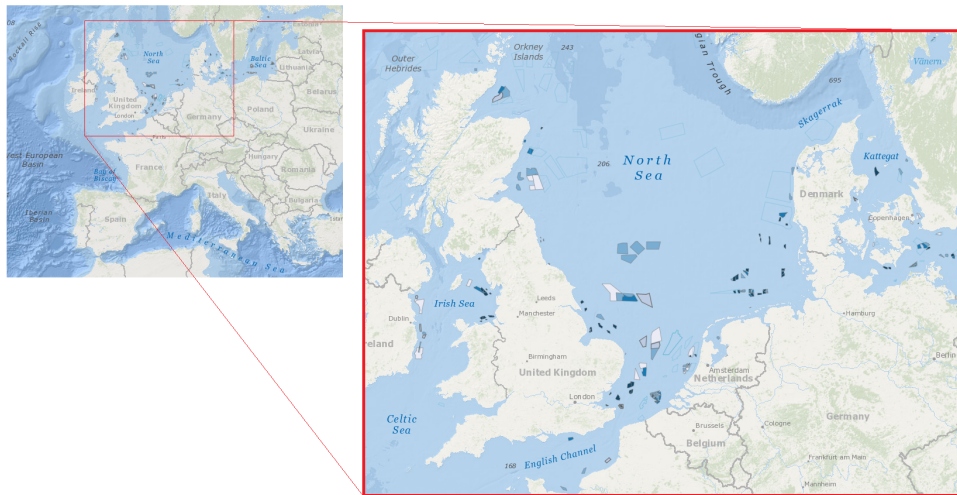


Figure 1.2: Offshore wind farms located in the North Sea.

1.1.3. OFFSHORE WIND TURBINES

The industry has been experimenting with the design of on- and offshore wind turbines in order to optimize the efficiency and costs. Although there are still numerous designs on the market, the basic configuration is the same for most turbines (Fig. 1.3). The general design of an offshore wind turbine can be sub-divided into three components:

- WTG (Wind Turbine Generator)
- transition piece
- support structure.

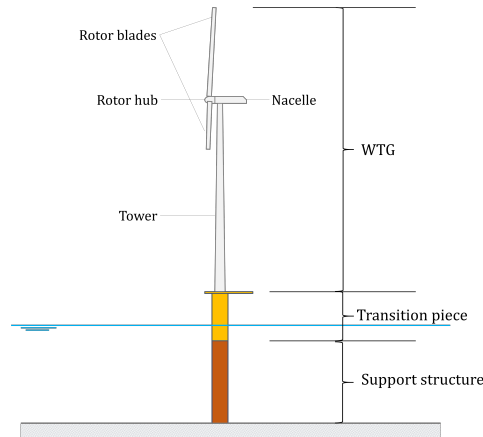


Figure 1.3: Graphical representation of the different components of an offshore wind turbine.

WTG

The wind turbine generator (WTG) of a wind turbine is the part used for generating electricity. The familiar looking WTG of a wind turbine consists of a tower, nacelle, rotor hub and rotor blades (Fig. 1.3). The rotor blades, which are connected to the rotor hub, drive the turbine's main shaft. Via gearboxes the main shaft is connected to a generator. The nacelle forms the casing to house/protect the turbine's delicate equipment.

TRANSITION PIECE

The transition piece forms the connection between the support structure (or foundation) and the WTG of the wind turbine. The transition piece often consists of a boat landing, a platform for maintenance workers and a small crane to handle cargo and to provide a way of fast evacuation for the maintenance crew. Furthermore, the transition piece forms a watertight casing for electrical components.

SUPPORT STRUCTURES

The function of the support structure is to secure the wind turbine to the ground; to prevent the turbine from tumbling over during its lifetime. As offshore wind turbines are often facing harsh conditions, the support structure must be able to withstand the substantial environmental loading acting on the structure. Depending on the water depth, soil conditions, wind turbine dimensions and costs, a choice must be made between different types of support structures. The most commonly used types of support structures are the monopile, jacket-, gravity based- and tripod structures as presented in Fig. 1.4. As can be seen from Fig. 1.4 the spreaded foundations (jacket, tripod) are used for deep water installations, whereas the monopile and gravity based foundations are often preferred in shallower water depths.

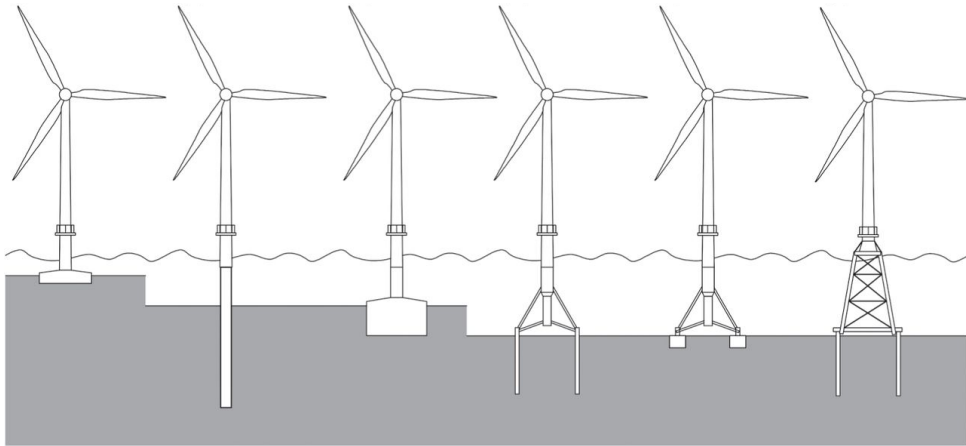


Figure 1.4: Offshore wind turbine support structures. From left to right: gravity based, monopile, caisson, multi-pile, multi-caisson and jacket

TURBINE CAPACITY

The increasing demand for renewable energy in combination with improving technologies contributes to the upscaling of wind turbine dimensions. Since the installation of the first offshore wind turbines, having a nominal power output of 450 kW, turbine sizes have been increasing. Currently installed wind turbines have power outputs up to 8-9 MW, where in the near future turbines of 12 MW and more are to be expected. Fig. 1.5 shows an overview of the increase in both turbine capacity and rotor diameter of offshore wind turbines over time.

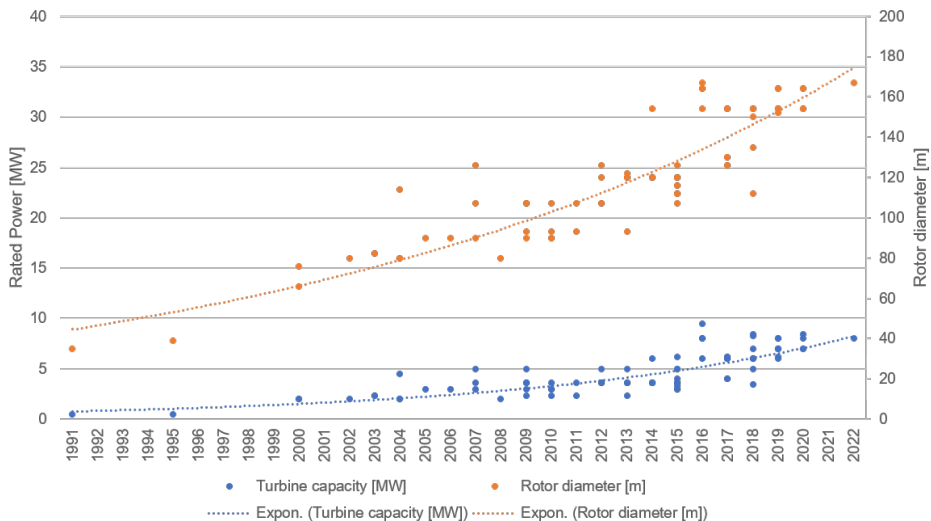


Figure 1.5: Increase of offshore wind turbine dimensions over time (turbine data from UK, NL, DE and DK).

1.2. TURBINE INSTALLATION

1.2.1. INSTALLATION PROCEDURE

The majority of the offshore wind turbines is being installed using jack-up vessels. The procedure of installing turbine components with a jack-up vessel (Fig. 1.6) is as follows. First, the turbine components are loaded onto the vessel after which it sails to its destination. Arriving at the windfarm, the jack-up starts its up-jacking procedure. When the vessel is elevated out of the water, the lifting operation can be conducted. After installation, the vessel lowers itself back into the water and moves on to start the next installation job. The main advantage of this procedure is the absence of vessel motions influencing the lifting operation. Some disadvantages of this concept are the time required for the jacking procedure and the jack-up's dependency on the soil conditions in finding a suitable foundation.

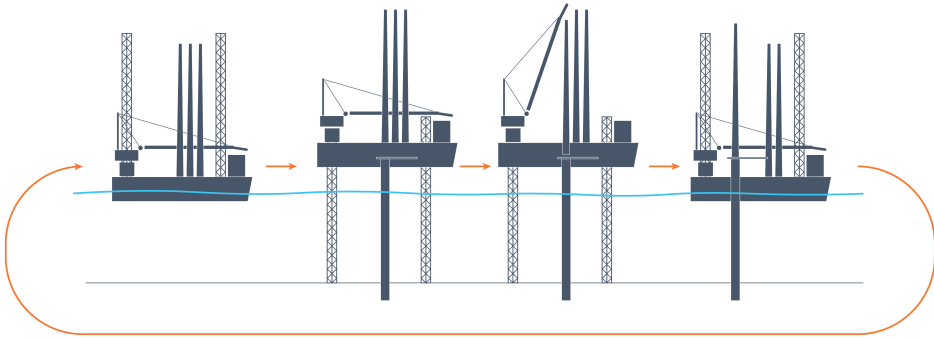


Figure 1.6: Installation sequence jack-up vessel.

1.2.2. TURBINE INSTALLATION VESSELS (TIVS)

The offshore wind market is a relatively new market and therefore prone to innovations and optimization of processes. In this section an introduction to state-of-the-art equipment and upcoming developments will be given. Hereby the focus will be on vessels used for the installation of offshore wind turbines.

JACK-UPS

The first jack-up vessel has been introduced to the offshore market in 1954. Originally jack-up vessels, or jack-up rigs, were used to carry out drilling operations in the oil- and gas industry. The upcoming offshore wind market drew the attention of numerous oil- and gas contractors, thereby introducing technologies from the oil- and gas to the offshore wind industry. In 2003 the construction of the Mayflower Resolution, world's first turbine installation vessel (TIV), was completed. Up to this day, jack-up vessels are the most common choice for in-field installation/maintenance of offshore wind turbines. Fig. 1.7 shows two jack-up vessels during installation of wind turbine components.



Figure 1.7: Two generations of jack-up vessels; MPI Resolution [l], Seajacks Scylla [r]

As discussed, the jack-up vessel is a very convenient tool for the installation of offshore wind turbines. A downside of the jack-up vessel, however, are the costs. According to TWD, the jack-up day rate is estimated to be >€150.000/day. As jack-up vessels have limited deck-space and need to jack up and down for each installation job, the total project costs can become quite significant. The current trends, to install turbines in deeper water depths and to install bigger turbines, will result in an increase of the jacking time and a limitation of the loading capacity. As this results in longer installation times, the operational costs will also increase.

SPECIALIZED VESSELS

As of lately, engineering firms have been introducing concept vessel designs to the market, most of them focusing on the installation of pre-assembled turbines. Vessels, like presented in Fig. 1.8, will potentially reduce the time required to install offshore wind turbines since jacking operations are no longer required. However, as a result from this, the vessel motions must be taken into consideration during installation.



Figure 1.8: Dedicated turbine installation concepts; Huisman [l], IHC Vuyk [m], Ulstein [r]

HEAVY LIFT VESSELS (HLVs)

Heavy lift vessels are widely used in the marine- and offshore market for the transportation and installation of heavy cargo. The large deck space and high lifting capacity (>3000t) make these vessels suitable for the installation of future generation offshore turbines. As of lately, the offshore wind market is developing a growing interest in these vessels for the installation of XXL monopiles. Whereas some contractors aim for specialized 'out of the box' solutions, other contractors have been ordering the design and construction of heavy lift vessels (Fig. 1.9). However, heavy lift vessels are not yet operational in the

offshore wind turbine installation industry. The introduction of vessel motions to the installation procedure changes the nature of the process; research must be conducted into this area.



Figure 1.9: Orion (DEME) [l], Bokalift 1 (Boskalis) [r]

1.2.3. PROPOSED FUTURE OF THE TURBINE INSTALLATION VESSEL

The vessels, as discussed in this section, are in theory all suitable for the installation of offshore wind turbines. The jack-up vessel has been a proven and improving concept since the first offshore wind farm has been installed. The absence of vessel motions during lifting operations makes it perfect for the installation of offshore wind turbines. However, jack-up vessels are known to have very high day rates and operation is limited by the water depth and soil conditions.

The 'specialized vessels' have one goal only: installation of wind turbines. The vessels are designed to install a completely pre-assembled WTG in one take, making them very effective. However, vessel motions have to be taken into account during installation and the deckspace is limited.

Heavy lift vessels have large deckspaces and are outfitted with high capacity cranes. The high capacity crane and large deckspace make them suitable for installing offshore wind turbines. However, as for the 'specialized vessels' vessel motions have to be accounted for.

An overview of the pros and cons of the different vessel types is presented in Table 1.1.

Table 1.1: Comparing the different turbine installation vessels.

	Pros	Cons
Jack-up vessels	+ no vessel motions + proven concept + easy operation	- dependency on soil conditions - small deck area - limited crane capacity - high day rates
Specialized vessels	+ pre-assembled wind turbines + short installation times + no jacking operations required + independent of soil conditions + (potential) high sailing speeds	- complex control systems - vessel motions - limited loading capacity - large structures on board - position keeping system required
Heavy lift vessels	+ high capacity cranes + independent of soil conditions + no jacking operations required + large deck-area + high sailing speeds + relatively low day rates + installation of foundations and WTGs	- complex control systems - vessel motions - position keeping system required

Looking at the pros and cons of each vessel type, the HLV seems very suitable for the installation of offshore wind turbines. However, research is required to find a solution to control the load during installation.

1.3. LOAD CONTROL DURING OFFSHORE OPERATIONS

While working at sea one must always be aware of the dynamic environment in which the work is done. Constantly changing conditions could even turn the simplest of operations into real, and potentially life threatening, obstacles. Heavy lift operations, installation jobs and the transfer of people to their daily working environment are operations that should be handled with great care. To ensure safe working, operations like these are often tied to small weather windows thereby increasing the risk of project delays.

Applying a form of motion compensation to the system can increase the operational window, improve the operational safety and reduce the weather downtime. Nowadays, there are numerous different motion compensation systems available on the market, both active- and passive. The difference between an active and a passive compensation system is the amount of control that is required to mitigate the motion. Where an active system is continually managed by a control system, passive compensation systems are 'passively' storing the energy induced by the external forces in the system. Frequently used components in both systems are winches and hydraulic cylinders.

A brief introduction to some of these systems, used in the offshore wind industry, is presented below.

1.3.1. PASSIVE SYSTEMS

BUMPERS/GUIDES

Bumpers/guides are used to guide the load into position. Common applications of guide systems in the offshore (wind) industry are steel funnels to force the load into position, pile extensions or bumpers to stop the motion of the load in a specific direction (Fig. 1.10). As mentioned, guiding systems can add some extra controllability during the positioning stage, however a significant amount of control is already required to begin with.



Figure 1.10: Guiding a lifted object during installation jobs; human guidance [l], guiding funnels/holes [m], guiding piles [r]

CRANEMASTER

The Cranemaster (Fig. 1.11) is a passive heave compensation system used during lifting operations where vessel motions are to be considered. The Cranemaster system acts as a shock-damper to reduce the peak loads during a lifting operation and to mitigate the motions of the load in the crane. Passive heave compensation uses a hydraulic accumulator (a pressurized container containing both gas and liquid) to store and release hydraulic energy.

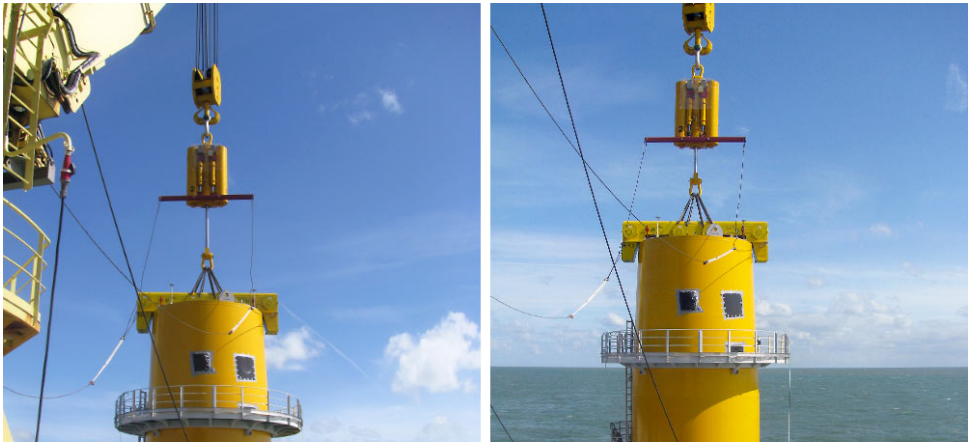


Figure 1.11: Cranemaster used for lifting a transition piece.

1.3.2. ACTIVE SYSTEMS

TUGGER/TAG LINES

Tugger/tag lines are commonly used during lifting operations, both on- and offshore, to reduce the rotation of the lifted object. Tugger/tag lines are attached to the load or lifting gear and are operated either manually or automatically. Tugger/tag lines can only be used to apply tension, so to increase the amount of control on the object the lines should be pretensioned. By actively controlling the tension on the lines, the horizontal movements and rotations of the load can be controlled quite accurately. Controlling the tension in the lines is often accomplished using (hydraulic) winches (Fig. 1.12).



Figure 1.12: Usage of taglines during lifting; manual control [l], attached to lifting gear [m], automatically controlled system [r]

MOTION COMPENSATED PILE GRIPPER

The motion compensated pile gripper, as presented in Fig. 1.13, has been introduced to the market to assist by the installation of monopiles from a floating vessel. The motion compensated pile gripper keeps the motions of the pile within certain limits during all phases of the installation. The motion compensated pile gripper, as designed by Temporary Works Design, ensures safe working up till a significant wave height of 2.5 m and within a horizontal plane of +/- 3.5 m.

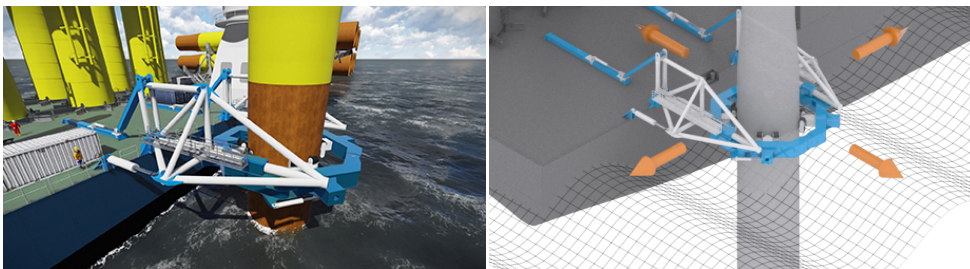


Figure 1.13: Motion compensated pile gripper.

3D MOTION COMPENSATED CRANES

The motion compensated crane is already in use in the offshore wind market. Cranes like this often consist of an active motion compensation system which compensates the heave, roll and pitch motions. Nowadays, motion compensated cranes are used for load transfer from a vessel to a stationary object (Fig. 1.14). The current generation of motion

compensated cranes is limited by its lifting capacity and size. Up till now, there are no motion compensated cranes on the market capable of completing turbine installation jobs.

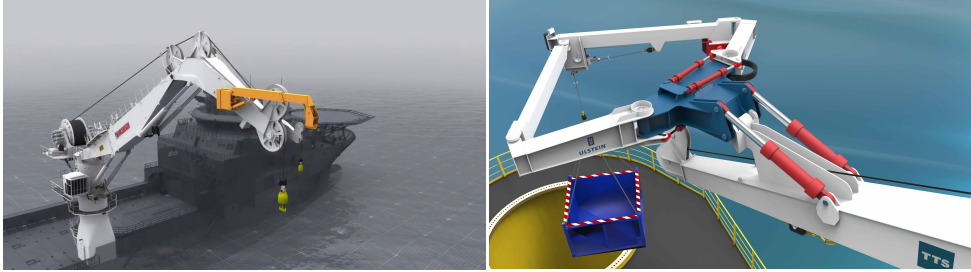


Figure 1.14: Current generation of motion compensated cranes, MacGregor [l], Ulstein [r].

1.4. OFFSHORE WIND; THE EXPECTATIONS

Anno 2018, jack-up vessels are the most convenient vessels to use for the installation of offshore wind turbines. However, due to an increasing demand for renewable energy the dimensions of wind turbines keep growing, thereby creating the need to reconsider the current methods of installation. The expectation is that in a few years' time, it will no longer be possible to install the new generation wind turbine components using the current installation vessels. The main reasons for this expected inability are the increasing turbine dimensions and the lack of crane capacities.

In theory, floating vessels are better suited to handle the upcoming developments in the offshore wind market than jack-up vessels. From Sec. 1.2.3 it has already become clear that it would be interesting to consider the possibility of installing offshore wind turbines using a floating installation vessel. Especially since an increasing number of offshore wind contractors ordered the construction of a large heavy lift vessel (HLV), presumably for future use in the installation of wind turbine components. Therefore, research must be conducted to determine the viability of floating installation and the effect the vessel motions will have on the installation of offshore wind turbines.

2

RESEARCH OBJECTIVE

From Ch. 1 it has become clear that the offshore wind market is a fast-growing market. As a result of the rising demands for renewable energy, market processes can be optimized thereby allowing turbines to become bigger in size. The use of current installation techniques may not be self-evident in the near future and therefore, the use of alternative methods should be examined.

In the previous chapter, floating installation has been opted as a good alternative for the installation of new generation turbines. At the moment of writing, the market is already experimenting with floating installation of large monopiles using HLVs.

As using floating installation vessels to install offshore wind turbines brings a new facet to the market, numerous new challenges have to be overcome. The influence of the vessel motions during installation is expected to be significant, and ways to mitigate the motions of the load in the crane to within safe working limits are to be found.

The focus of this thesis will be on the installation of wind turbine towers using a HLV.

2.1. RESEARCH OBJECTIVE

It is in TWD's interest to develop an efficient solution with the ability to safely install wind turbine towers from a HLV. To assess both the technical and economic viability of installing wind turbine towers using a floating vessel, the following research objectives must be fulfilled.

Find the most efficient way to control the motions of the wind turbine tower to within safe working limits during installation using a HLV, when taking into account the motions as a result of the environmental conditions.

To accomplish this objective, the problem is divided into multiple sub-objectives. Finding answers to these sub-problems will provide a good reference frame to achieve the main objective. The sub-objectives are:

- List the main benefits of installing towers using a HLV
- Introduce concepts that allow safe installation of towers using a HLV
- Create a simplified model to find the optimal installation method
- Create an Orcaflex model to test the tower response using the optimal installation method

2.2. SCOPE AND AIM

Since there is no real reference or guide regarding the floating installation of wind turbine components, one should first identify the potential problems that could be encountered. To do so, the installation process could either be considered the lifting and installation of a single turbine or the complete process of installation, including loading and transfers. To make the entire operation more cost efficient, one should consider the installation process as a cycle (see Fig. 2.1). However, before optimizing the entire process a closer look should be taken at the possibility of safely installing a single turbine.

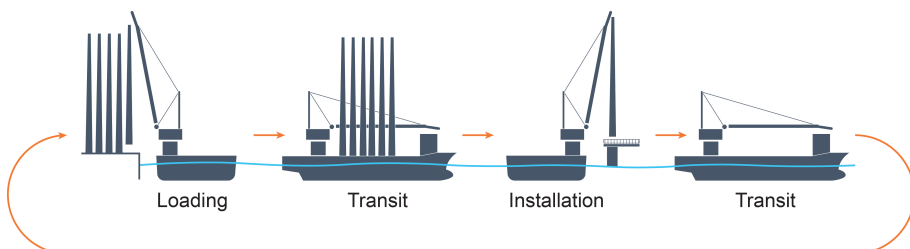


Figure 2.1: Installation cycle

The process of installing a single turbine can be divided in multiple phases. Examining the isolated installation process, as visualized in Fig. 2.2, in more detail, the following sub-problems/installation phases can be identified:

1. lift-off from sea fastening;
2. moving of tower to transition piece;
3. positioning tower above transition piece;
4. touchdown of tower on transition piece;
5. releasing tower.

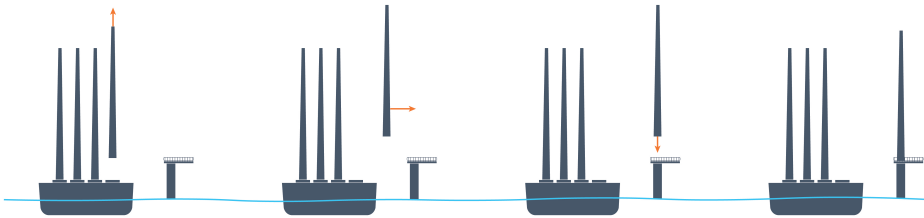


Figure 2.2: Installation phases. From left to right: lift-off from sea fastening, move-out to TP, positioning above TP, touch-down on TP

The focus of this thesis will be to design a concept able of covering all the different installation phases. However, special attention is given to the positioning/touchdown of the tower above/on the transition piece, since the positioning/touchdown is believed to be the most critical phase of the installation.

2.3. THESIS OUTLINE

To provide the reader with a structured and chronologic overview of the encountered problems and the suggested solutions, the thesis is subdivided into multiple sections. Each chapter will create a handhold to understanding the problem and the decisions made during the different project phases. A complete overview of each chapter is given below.

Chapter 1 - Introduction provides an introduction to the offshore wind market. This chapter briefly touches the different components of which an offshore wind turbine consists, elaborates on the current method used to install offshore turbines and proposes alternative methods to install the future generation of offshore wind turbines.

Chapter 2 - Research Objective elaborates on the problem statement, the research objective and presents an outline of the thesis.

Chapter 3 - Functional Design focuses on the process of designing a solution allowing safe installation of towers using a floating heavy lift vessel. In this chapter a list of requirements and criteria is introduced that serves as a guide frame to justify the design considerations. Finally, the concepts are tested against the requirements and criteria using a multi-criteria analysis. Two concepts are selected that fulfill the initial requirements.

Chapter 4 - Vessel-Tower Model introduces a model to analyze the tower response in a general way. The model consists of a double pendulum with a moving support point. The content in this chapter focuses on the response of the tower in the crane. The system's EoMs are obtained using the Lagrange method. Initially, the response of a free hanging tower is considered in the frequency domain. Then motion compensation is added, represented by a (virtual) spring-damper connected to the fixed world. Using the results obtained with the frequency domain analysis, the response of the tower is minimized by optimizing the position, stiffness and damping of the compensation system. As analyzing a system in the frequency domain requires a system to be linear, the response of the tower is compared to time domain simulations to check the effect of linearization on the response.

3

FUNCTIONAL DESIGN

This chapter presents a brief overview of a conceptual study with the goal to design a tool that can safely install wind turbine towers using a floating vessel. As the study will remain on concept level, mechanical and/or structural aspects will not be treated. The solutions, as proposed in this chapter, are introduced to obtain a better insight in the installation process and to create a reference frame for the development of future products.

As discussed in Ch. 1, current installation vessels are expected unable of installing the new generation wind turbines. As an alternative, floating installation vessels are expected to gain popularity among the offshore wind contractors. Embedding these vessels into the industry brings new opportunities, but also introduces new challenges.

3.1. DESIGN STRATEGY

The design of an offshore structure, or any kind of structure, starts with a motivation. In the field of engineering, this motivation is often equivalent to a problem, which needs to be overcome to make life easy again. In other words, there is a need to solve a specific problem and therefore, the product should add value to the market by solving the problem in one way or the other. However, there might be a hundred or more different solutions to the problem. To find a suitable solution, guidance is used in the form of the Delft Design Guide ([van Boeijen and Daalhuizen, 2010]). The Delft Design Guide presents theories, strategies and tools which can be used for product design, with a special focus on engineering problems. A recurring theme in the guide is to reason from function to form, rather than the other way around. Although the form will always be subjected to practical considerations, the designer should not be held back too much.

3.1.1. ENGINEERING MODELS OF PRODUCT DESIGN

Engineering models of product design are developed to provide guidance and structure to the design process. In the Delft Design Guide, two models are discussed that follow the same structure: the Pahl and Beitz model and the Verein Deutscher Ingenieure model. Both models divide the design process in phases: problem analysis, conceptual design, embodiment design and detail design. A global overview of the model flow is presented in Fig. 3.1 below.

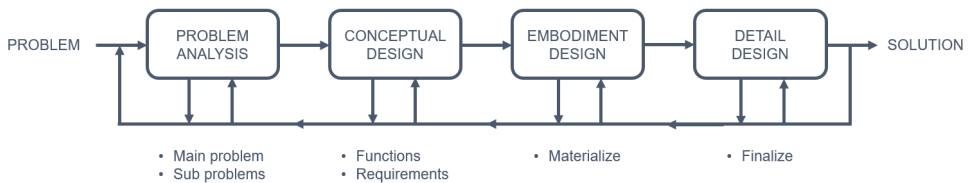


Figure 3.1: Model flow

One should start the design process with acquiring a clear interpretation of the problem during the problem analysis phase. This phase should contain an explanation of the main problem and the sub problems.

Then, in the conceptual design phase, after the problem is defined and analyzed, one can delimit the scope of the problem by introducing functions, requirements and criteria the design should be able to fulfill. Reasoning from function to form, whilst keeping in mind the requirements and criteria, one can start considering methods to handle the sub-problems.

At the ‘end’ of the conceptual design phase concepts are presented, which are given more form and thought in the embodiment design phase. In this phase the concept design gets more detailed resulting in, first, a preliminary design and finally a definitive design. At the end of the detail design phase, a design is obtained meeting all criteria and considerations.

The design process is a very dynamic process, work accomplished in one phase can influence considerations and assumptions made in earlier phases. Therefore, one must constantly re-evaluate the work done. In Fig. 3.1 the evaluation process is indicated using feedback loops between the different phases.

This thesis will go through the first two phases of the design process (problem analysis and conceptual design).

3.2. PROBLEM STATEMENT

Following the engineering models of product design, the design process should start with defining the problem. The research objective, presented in Ch. 2, states that a solution must be found that is able *to control the motions of the wind turbine tower to within safe working limits during installation in the most efficient way when using a HLV and thereby taking into account the motions as a result of the environmental conditions.* The value the design should add to the market can therefore be defined as: allowing safe installation of wind turbine towers from a HLV. The main function of the design, corresponding to this value, is to control the motions of the tower to within safe working limits.

As even small vessel motions can potentially result in large displacements of the tower during lifting, the main problem will be to mitigate the effect the vessel motions will have on the motion of the tower during installation, thereby keeping the tower motions to within specified limits. The installation process can be subdivided into multiple phases, which can be considered as sub-problems to the main problem statement.

3.2.1. SUB-PROBLEMS

As mentioned above, the problem of installing wind turbine towers, while taking the vessel motions into consideration, can be decomposed into a number of sub-problems. Each sub-problem should be solved in turn, as to finally obtain a concept that can handle every aspect of the problem.

The different sub-problems/installation phases were defined in Ch. 2 as:

1. lift-off from sea fastening;
2. moving of tower to TP;
3. positioning tower above TP;
4. touchdown on TP;
5. releasing tower.

In a first effort to delimit the endless research possibilities, the following preliminary project boundaries are introduced. According to the level of relevance, a distinction has been made between 'must haves' and 'nice to haves'.

Must haves

- heavy lift crane vessel
- vertical sea-fastening of towers

Nice to haves

- self-propelled vessel
- no major preliminary alterations to tower required
- installation of tower sections
- installation of both tower and nacelle
- vessel heading unrestricted

3

3.3. DESIGN REQUIREMENTS AND CRITERIA

In the preceding section the problem has been introduced and subdivided into a number of sub-problems. Boundaries have been introduced in a first effort to delimit the problem statement. To further constrain the problem, requirements and criteria are introduced. This section briefly discusses the framework of requirements the concept design has to comply with. The design requirements can be sub-divided into both general and functional requirements. When a concept design does not fulfill the requirements, it should either be modified or discarded.

The general requirements, presented below, are based on TWD's experience regarding client wishes. They are crucial for the working and marketing of the concept and as such, must not be forgotten.

GENERAL REQUIREMENTS

- allow the installation of wind turbine towers from a floating installation vessel
- ensure a safe working environment
- be more cost efficient than current installation methods
- be robust
- be suited for all the loads during the different project stages
- system is inboard during transit
- ensure easy handling

The functional requirements focus on the operational aspects of the problem. In the list of functional requirements the safe working limits are defined. These limits are proposed by TWD as a first guideline and are assumed to allow safe installation of the tower provided a bumper or guidance system is in place to further mitigate the displacements of the tower. An overview of the functional requirements is presented below.

FUNCTIONAL REQUIREMENTS

- assist tower during installation phases
 - lift-off from sea fastening
 - approach TP
 - touchdown on TP
- ability to handle different tower diameters (5 - 7 m)
- ability to handle different tower lengths (80 - 120 m)
- ensure the accuracy of the tower position (at TP) during installation to within:
 - horizontal: $x_{bot}, y_{bot} \pm 0.2$ m (MPM for a 3 hour simulation)
 - vertical: $z_{bot} \pm 0.1$ m (MPM for a 3 hour simulation)
- allow safe working up to the design parameters:
 - current up to 1.5 m/s
 - significant wave height up to 2.5 m
 - waveperiods 6 - 9 s
 - wind speeds up to 12 m/s
- designed to be compatible for future developments
- minimize loads on the tower

3.4. SUB-SOLUTIONS

The sub-problems, as specified above, combined with the design requirements are used to generate a solution to each sub-problem. The sub-solutions are the result of a number of 'braindraw' sessions with the business development team of TWD. The braindraw sessions are basically the embodiment of the reasoning from function to form principle and therefore, are very useful to generate ideas in the conceptual design phase. In sessions like this, it is important that a large amount of ideas is generated. During the braindraw session, ideas are sketched on a piece of paper rather than written down. After a while the papers are exchanged between the participating people. By exchanging the pieces of paper between the participants, participants are, in theory, motivated by and able to build on other people's ideas. After each session, all ideas are collected and sorted per sub-problem. Finally, a small selection of the sub-solutions can be presented (per sub-problem) in a morphological chart, see Fig. 3.2. Combining the sub-solutions, one can obtain a concept that is able to fulfill its function of controlling the tower motions to within safe working limits. The arrows in Fig. 3.2 are used to indicate logical connections between the sub-solutions.

Combining the different sub-solutions resulted in a total of five concepts that should be able to maintain the tower motions to within the specified limits and therefore allow the

safe installation of wind turbine towers from a floating vessel. The five concepts, that are discussed briefly in the section below, vary in working principle and complexity.

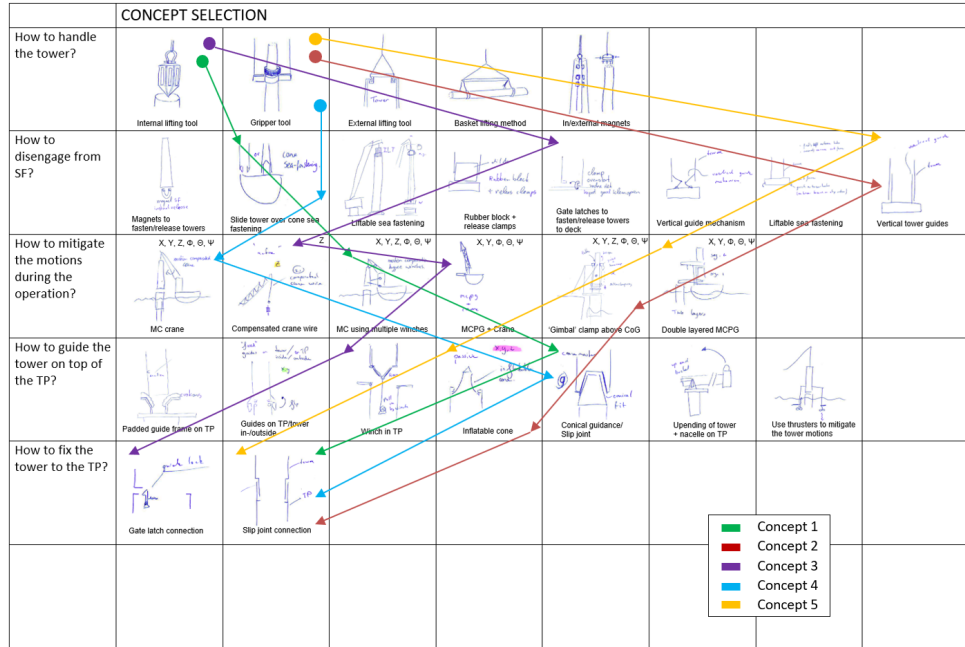


Figure 3.2: Morphological chart.

3.5. CONCEPTS

The concepts presented in this section are the first products of the conceptual design phase in which, using the braindraw sessions, ideas are generated to solve the different sub-problems. At this stage of the design process, the concepts are a conceptualized representation of the requirements and criteria, yet nothing is known about the structural aspects of the concepts. An overview of the concepts is presented below.

Concept 1: "Tugger Winches"

The first concept uses the crane's tugger winches to mitigate the tower motions. The winches can be attached to the tower at multiple locations to assist the tower during the installation process. As cables are not suitable to exert pushing forces, the cables should be pre-tensioned. The pre-tension allows the cable force to be increased or decreased such that an effective spring-damper characteristic can be used to minimize the tower motions. An impression of how a concept like this could look can be found in Fig. 3.3. The figure indicates multiple layers of winches connected to the tower representing the possibilities of this concept.

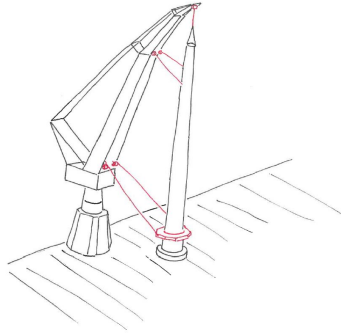


Figure 3.3: Concept 1: using cables to 'steer' the tower during lifting.

Concept 2: "Gimbal Clamp"

The second concept, as presented in Fig. 3.4, grabs the tower just above the tower's center of gravity to minimize rotations of the tower resulting from horizontal displacements. The vessel's heave motion is compensated by the hydraulic cylinders at the top of the tool. The ball joint, in combination with the hydraulic cylinders at the bottom of the tool, make it possible to mitigate the vessel's roll and pitch motions. The tool is able to grab the tower, therefore an onboard crane is no longer required to install towers.

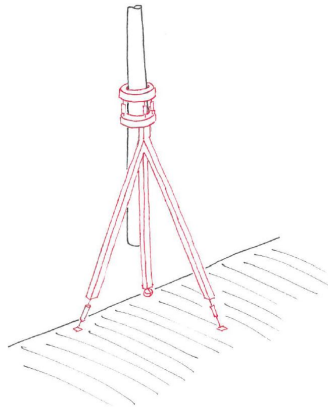


Figure 3.4: Concept 2: grabbing the tower around C.o.G..

Concept 3: "MCPG"

The third concept has been generated using already existing market assets. This concept uses TWD's motion compensated pile gripper to compensate for the vessel's horizontal movements. If required, the vertical motion of the crane tip can be mitigated by application of a Cranemaster/heave compensator in the top of the crane. A graphical representation of the concept is shown in Fig. 3.5.

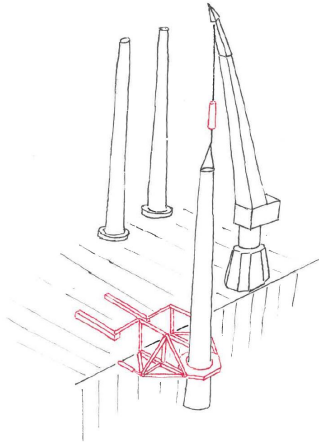


Figure 3.5: Concept 3: combining two existing motion compensation systems.

Concept 4: "3D Motion Compensated Crane"

Although motion compensated cranes have already been introduced to the offshore wind market, they have not been used for heavy installation jobs as the current lifting capacity is too small. A motion compensated crane would be an elegant solution to mitigate the environmental conditions but falls outside the company's scope. An artist impression of such a concept is given in Fig. 3.6.

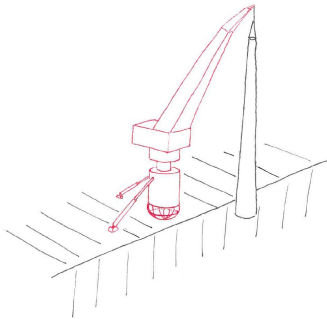


Figure 3.6: Concept 4: motion compensated crane.

Concept 5: "Double layered MCPG"

The fifth, and final, concept combines two motion compensated pile grippers (see Fig. 3.7). By mitigating the horizontal motions at two different positions along the tower height, the rotations as a result of the environmental conditions can be compensated. However, the interaction between the two systems can make this a complicated concept.

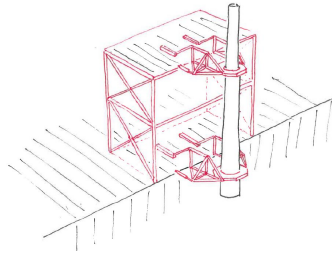


Figure 3.7: Concept 5: combining two motion compensated grippers.

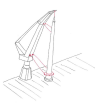

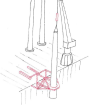

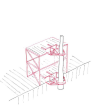
3.5.1. MULTI-CRITERIA ANALYSIS

The feasibility of each concept should be verified against a selection of design criteria. The criteria are introduced to test and compare concepts with one and another. An overview of the design requirements and criteria is presented below. There are eight main criteria of which some are divided into sub criteria.

- Design complexity
- Operational costs
 - Workability
 - Number of trips
 - Power consumption
 - Level of maintenance required
- Construction costs
 - Structural costs
 - Manufacturability (easy to build)
- Overall project duration
 - Installation efficiency
 - Operational cycle time
- Ability to install
 - Range of tower diameters and lengths
 - Tower sections
 - Both tower and nacelle
- Robustness
- Vessel independent
- Lifetime/durability

An effective way to test the design against the criteria is by applying a multi-criteria analysis. Weight factors have been assigned to all criteria to indicate the level of relevance of each criterion for the final product. Since the concepts at this stage are only a representation of the requirements and criteria, and no information about the structural aspects of the concepts is available, the ratings given to the concepts are partly based on TWD's experience and partly on assumptions.

Table 3.1: Multi-criteria analysis of the different concepts.

MCA	Weight factor					
Ranked from 1 to 5		Concept 1	Concept 2	Concept 3	Concept 4	Concept 5
Design complexity	2	++	±	±	-	-
Operational costs						
Workability	4	+	+	+	++	+
Number of trips	2	+	+	±	+	-
Power consumption	3	++	++	±	-	++
Maintenance required	1	++	-	-	-	-
Construction costs						
Structural costs	2	\$	\$\$	\$\$\$	\$\$\$\$	\$\$\$\$
Manufacturability	4	++	+	±	-	-
Overall project duration						
Installation efficiency	4	±	+	±	+	-
Operational cycle time	4	+	+	+	++	-
Ability to install						
Various tower dimensions	5	++	++	++	++	+
Tower sections	1	+	-	-	++	++
Tower and nacelle	5	-	+	-	-	-
Robustness	4	-	+	-	+	-
Vessel independent	2	+	+	++	-	-
Lifetime/durability	3	-	+	+	+	+
Weighed total		168	186	146	141	103

Each rating in Table 3.1 can be assigned a value ranging from 1 to 5 by applying the scaling factors presented in Table 3.2. The weighed total is the sum of the individual ratings.

Table 3.2: Scaling factors used to score the concepts.

General	-	-	±	+	++
Costs	\$\$\$\$	\$\$\$\$	\$\$\$	\$\$	\$
Weight	1	2	3	4	5

Looking at the results of the multi-criteria analysis, it becomes clear that the Gimbal Clamp concept (concept 2), the Tugger Winch concept (concept 1) and the MCPG concept (concept 3) are the most preferable. Furthermore, one can see that the ability to install different tower dimensions and the ability to install both tower and nacelle are considered important for the design. However, most concepts score bad on the nacelle installation since a different way of lifting would be required for installation of turbine

and nacelle in one part.

In Sec. 3.2.1 project boundaries are listed in the form of ‘must haves’ and ‘nice to haves’ as a first effort to delimit the research possibilities. These boundaries reflect, in theory, the initial wishes of the client regarding the outline of the design. The first ‘must have’ boundary states that a concept is to be used in combination with a heavy lift crane vessel. The Gimbal Clamp concept (concept 2), however, is designed to work without an onboard crane. Therefore, in accordance with the client’s scope and in consultation with TWD, the choice has been made not to analyze the performance of the concept in this thesis.

Although the motion compensated crane is believed to be a very effective solution to the problem, it scores relatively low in the multi-criteria analysis. This can be attributed to both the complexity of such a design and the high development costs. The motion mitigating abilities of the crane are expected to be very good, thereby assuming the displacements of the crane tip to be nihil, resulting in small tower responses. Manufacturers of offshore equipment, like Huisman, already announced their means of introducing a motion compensated crane to the market suitable of installing offshore wind turbines. As the motion compensated crane concept is considered a serious competitor to any installation concept introduced by TWD, it can be used as a ‘base case’ to test the concepts.

3.6. CONCEPT PERFORMANCE

The concept solutions, presented in this chapter, differ in size, working principle, complexity and many more. Although the concept solutions, in theory, should all be able to fulfill their function of controlling the tower motions to within the specified boundaries, further research is required to test the performance of the concepts. However, in this stage of the research the concepts do not yet resemble much more than an artist impression. In reality, the system’s geometric- and structural properties (stiffness, damping, weight, etc.) play an important role in the performance of the system.

Before continuing and working out concepts in more detail in the embodiment design phase, it would be interesting to know if it is possible to control the tower motions to within the specified limits by applying a form of motion compensation. Since, at this stage of the project, no information about the structural aspects of the concepts is available, a generalized model is used to compute the tower response under the assumption of a perfect motion compensation system.

In its simplest form, a motion compensation system can be represented as a (virtual) spring-damper system. A more detailed explanation of why and how the motion compensation system can be represented as a (virtual) spring-damper system is presented in Sec. 4.3.5. By representing the system as a (virtual) spring-damper rather than a complex system of hydraulic cylinders, an initial estimate of the stiffness and damping, required to mitigate the tower response, can be made. Although the spring-damper system does not directly resemble one of the concepts, the results can be used in a more general sense to analyze the concepts. As the concepts each ‘grab’ the tower at different positions

along the height of the tower, it will be interesting to analyze the effect of positioning the spring-damper system at different positions along the height of the tower.

The results from an analysis like this can be used to perform a design iteration step, by re-evaluating the concepts (see Appendix A).

4

VESSEL-TOWER MODEL

In Ch. 3 a method has been proposed to analyze the response of the tower in the crane in a general way by representing the motion compensation as a virtual spring-damper system. This chapter introduces a model to examine the response of the tower with and without the influence of the motion compensation system. The first step is to analyze the response of the system in the frequency domain. By changing the position of the motion compensation system along the height of the tower, the position of the motion compensation system can be found for which the response is minimized. Finally, the response of the tower is analyzed in the time domain using the static- and dynamic analysis software package Orcflex.

4.1. REFERENCE FRAMES

A simplified 3D representation of the vessel is presented in Fig. 4.1, where a system of four right-handed axes systems is introduced to indicate the positions of the vessel and tower with respect to each other and with respect to a fixed point on earth.

The first axis system $0(x_0, y_0, z_0)$ is fixed relative to the earth and is used to determine the position of an object with respect to a fixed point. Since the TP/monopile configuration is fixed to the earth, the influence of waves and current on the bending of the TP/monopile configuration can be ignored and both the vessel and tower position with respect to the TP are important, the origin of the fixed reference system is located at the center line of the TP. The x,y-plane of the axis system coincides with the still water level and the z-axis is positioned upwards.

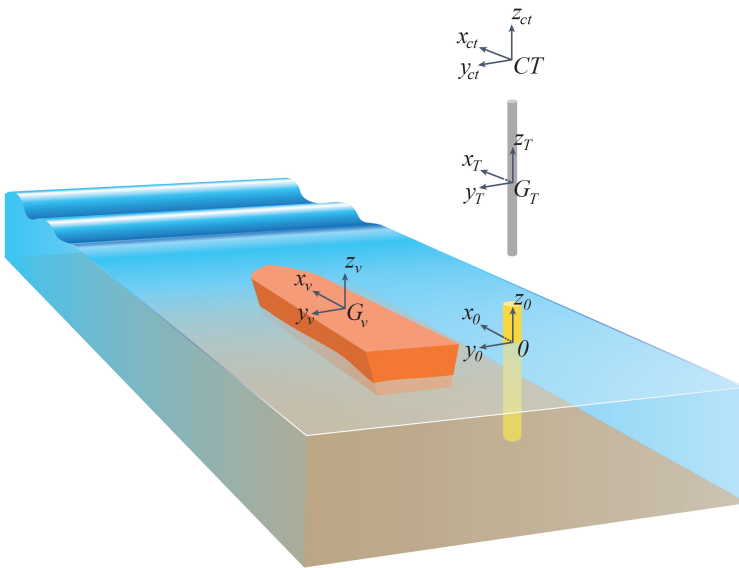


Figure 4.1: Reference frame.

The second axis system $G_v(x_v, y_v, z_v)$ is fixed to the vessel and is used to describe the movement of the vessel with respect to the fixed axis system. The origin of the vessel bound axis system is positioned in the C.o.G. of the vessel.

To describe the rigid body motions of the tower structure in a convenient way, the third axis system $G_T(x_t, y_t, z_t)$ is bound to the tower. The origin of the tower bound axis sys-

tem is positioned in the C.o.G. of the tower.

Finally, one might be interested in the way the crane tip moves with respect to the vessel and the fixed reference point. Therefore, the fourth axis system $CT(x_{ct}, y_{ct}, z_{ct})$ is bound to the crane tip position.

The initial positions of the axis systems, as used in thesis, with respect to the fixed axis 0 are:

$$\begin{aligned} G_v(x_v, y_v, z_v) &= (0.0, 46.0, 0.2) \\ G_T(x_T, y_T, z_T) &= (0.0, 0.0, 80.0^*) \\ CT(x_{ct}, y_{ct}, z_{ct}) &= (0.0, 0.0, 170.0) \end{aligned}$$

* The height of G_T varies for different tower dimensions and different installation phases.

4.2. VESSEL MODEL

This section introduces the vessel used for the simulations, the vessel's response to incoming waves and provides insight in how to determine the motions of an arbitrary point on the vessel.

4.2.1. VESSEL CONVENTIONS

With the axis systems defined, one can specify the vessel motions (both translations and rotations) about the axis. The three translations, described below, are considered positive along the axis, whereas the three rotations are defined conform the definitions of a right-handed axis system. The six vessel motions are *surge*(x), *sway*(y), *heave*(z), *roll*(ϕ), *pitch*(θ) and *yaw*(ψ); see Fig. 4.2 for a graphical representation of the six motions.

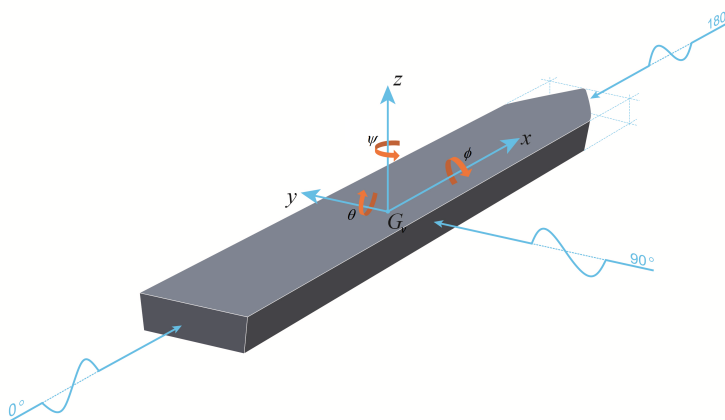


Figure 4.2: Definition of the vessel motions.

Looking along the positive x-direction, the right- and left-hand side of the vessel are called starboard- and portside respectively. In the same orientation, the front and back of the vessel are called the bow and stern.

Finally, the directions in which environmental disturbances such as waves, wind and current are propagating towards the ship must be clarified. The direction in which the environmental disturbances act on the vessel is of major importance for the performance of the vessel. The definition of the incoming wave direction is presented in Fig. 4.2 for three directions. Waves travelling from bow to stern along the length of the ship are called headwaves, waves travelling in the opposing direction are called sternwaves and waves travelling from starboard to portside or from portside to starboard along the width of the ship are called beamwaves.

4

4.2.2. SIMULATION VESSEL

In accordance with Ch. 1, the vessel used for the simulations is a HLV with parameters as specified in Fig. 4.3. The simulation vessel shows great similarities to the vessel presented in Fig. 4.3. The on-board crane, positioned at the starboard side of the vessel, has a lifting capacity of approximately 3000 tons.

Parameters	
Lpp	213 m
B	46 m
T	8 m
Δ	53567 t




Figure 4.3: Vessel similar to the simulation vessel.

4.2.3. VESSEL MOTIONS

As discussed in Sec. 4.2.1, the vessel's response to environmental disturbances can be described as a combination of three translations (surge, sway and heave) and three rotations (roll, pitch and yaw). The dynamics of a vessel depend on multiple factors, such as the shape of the vessel, the environmental conditions and the operational conditions.

Following Newton's second law one can derive the equations of motion for each degree of freedom by setting the sum of the external forces acting on the vessel equal to the vessel mass times its acceleration (Eq. 4.1).

$$\begin{aligned}
 m\ddot{x}_i &= \sum F_{e,i} & \text{for } i &= 1, 2, 3 \\
 J\ddot{x}_j &= \sum M_{e,j} & \text{for } j &= 4, 5, 6
 \end{aligned} \tag{4.1}$$

Where the equations appointed i index represent the translational directions and the equations indexed j represent the rotational degrees of freedom.

The external loads acting on a vessel can be categorized as hydromechanic- and wave exciting forces and moments. The hydromechanic loads are loads originated by an oscillating movement of the vessel in still water conditions, whereas the wave exciting loads find their origin by waves impacting a restrained body.

The hydromechanic loads can be obtained by experiment and measurement. When removing the vessel from its equilibrium state by giving it an initial displacement, the vessel will be subject to a restoring force ($-c_v \dot{x}_i$) equal to the additional volume of water displaced by the vessel. This force tends to push the vessel back to its equilibrium position, resulting in either a translational or rotational motion of the vessel. Apart from the restoring force, the vessel is exposed to hydrodynamic reaction forces proportional to the acceleration ($-a_v \ddot{x}_i$) and the velocity ($-b_v \dot{x}_i$) of the vessel. Waves are generated, due to the movement of the vessel, which propagate away from the vessel, thereby dissipating energy from the system. This dissipation of energy is represented by the damping force $-b_v \dot{x}_i$.

The wave exciting loads are the result of waves colliding with a restrained vessel. The wave exciting loads can be divided into two components: the Froude-Krylov force and the diffraction force. The Froude-Krylov force is defined as the time-varying part of the pressure integrated over the submerged hull area. To calculate the Froude-Krylov force, it is assumed that the time varying part of the pressure along the hull results from an undisturbed wave propagating along the length of the hull. As this is a rather conservative approach, a correction on the Froude-Krylov force is proposed in [Journée et al., 2015] taking into account the diffraction of waves by the vessel.

Summation and rearrangement of all terms results in Eq. 4.2, where F_h , F_{FK} and F_d are the hydromechanic-, Froude-Krylov- and diffraction forces. Although the equations presented below account for the translational motions, the same principle can be applied for the rotational degrees of freedom.

$$\begin{aligned} m\ddot{x}_i &= F_h + F_{FK} + F_d \\ m\ddot{x}_i &= -a_v \ddot{x}_i - b_v \dot{x}_i - c_v x_i + a_v \ddot{\zeta}^* + b_v \dot{\zeta}^* + c_v \zeta^* \\ (m + a_v)\ddot{x}_i + b_v \dot{x}_i + c_v x_i &= a_v \ddot{\zeta}^* + b_v \dot{\zeta}^* + c_v \zeta^* \end{aligned} \quad (4.2)$$

Considering a real system, six equations of motion are obtained: one for each degree of freedom. For clarification, this system of equations may be written in matrix form as presented in Eq. 4.3.

$$(M + A(\omega))\ddot{X} + B(\omega)\dot{X} + CX = F(\omega) \quad (4.3)$$

Where $X = (x, y, z, \phi, \theta, \psi)^T$ and the matrices M , A , B and C are the mass, added mass, damping and stiffness matrices respectively.

4.2.4. RESPONSE IN WAVES

For linear systems, one can describe the response of a vessel to an incoming wave using complex transfer functions. In such a case, the transfer function contains information about the magnitude of response to an incoming wave and the phase difference between the response motion and the incoming wave. In general, a transfer function provides a compact description of the input-output relation for a linear system [Åström and Murray, 2008].

The system of Eq. 4.3 can be re-written using the complex transfer function notation. A frequency domain representation of this system is presented in Eq. 4.4, where H_{fi} is the complex transfer function relating the external forces to the sea surface elevation.

$$(-\omega^2(M + A(\omega)) + i\omega B(\omega) + C)X_i = H_{fi}(\omega)Z \quad (4.4)$$

The expression in Eq. 4.4 can be re-written to obtain the displacement amplitude as a function of the complex force transfer function, the inertial forces and the sea surface elevation (Eq. 4.5). Finally, one can derive the complex transfer function that relates the motion of the vessel to the sea surface elevation (Eq. 4.6).

$$X_i = \frac{H_{fz,i}(\omega)}{(-\omega^2(M + A(\omega)) + i\omega B(\omega) + C)}Z \quad (4.5)$$

$$H_{xi}(\omega) = \frac{X_i}{Z} = \frac{H_{fz,i}(\omega)}{(-\omega^2(M + A(\omega)) + i\omega B(\omega) + C)} \quad (4.6)$$

The complex transfer function relating the response motion to the change in sea surface elevation is, in literature, also known as the Response Amplitude Operator (RAO) (see Eq. 4.7). The real part of the RAO relates the amplitude of the response to the amplitude of the sea surface elevation, whereas the imaginary part can be used to relate the phases of both signals.

$$H_{xi}(\omega) = \frac{X_i}{Z} = RAO_i(\omega) \quad (4.7)$$

4.2.5. RESPONSE OF CRANE TIP

For a linear system (assuming small angles), the response of an arbitrary point on the vessel can be determined by superposition of the C.o.G. motions of the vessel to the location of the arbitrary point. The position of the crane tip with respect to the vessel C.o.G. is defined as $CT_{CoG} = (CT_x, CT_y, CT_z)$. Then, the translations of the crane tip can be determined using Eq. 4.8.

$$\begin{aligned} x_{ct} &= x + CT_z\theta - CT_y\psi \\ y_{ct} &= y - CT_z\phi + CT_x\psi \\ z_{ct} &= z + CT_y\phi - CT_x\theta \end{aligned} \quad (4.8)$$

The system of equations, presented above, can be written in matrix notation as:

$$X_{ct} = TX \quad (4.9)$$

Where T is the transformation matrix containing the crane tip coordinates.

$$T = \begin{bmatrix} 1 & 0 & 0 & 0 & CT_z & -CT_y \\ 0 & 1 & 0 & -CT_z & 0 & CT_x \\ 0 & 0 & 1 & CT_y & -CT_x & 0 \end{bmatrix} \quad (4.10)$$

Then, replacing the motion components in Eq. 4.9 by X_{ct}/Z and X_i/Z one can determine the RAO relating the motions of the crane tip to the amplitude of the waves.

$$\frac{X_{ct}}{Z}(\omega) = T \frac{X}{Z}(\omega) = RAO_{ct}(\omega) \quad (4.11)$$

A graphical representation of the crane tip RAOs, for an incoming wave direction of 180 degrees, is presented in Fig. 4.4. Looking at this figure, one may observe that even for an incoming wave direction of 180 degrees, the crane tip describes a swaying motion. This can be explained by the fact that the C.o.G. of the vessel is positioned slightly off-center. The vessel RAO has been constructed for the vessel including a monopile gripper, causing the position of the C.o.G. to shift. Nevertheless, this RAO is used for the simulations due to a lack of better data. Since the crane tip is positioned approximately 170 m from the vessel C.o.G. in z-direction, a small roll angle can lead to a significant swaying motion of the crane tip (Eq. 4.8).

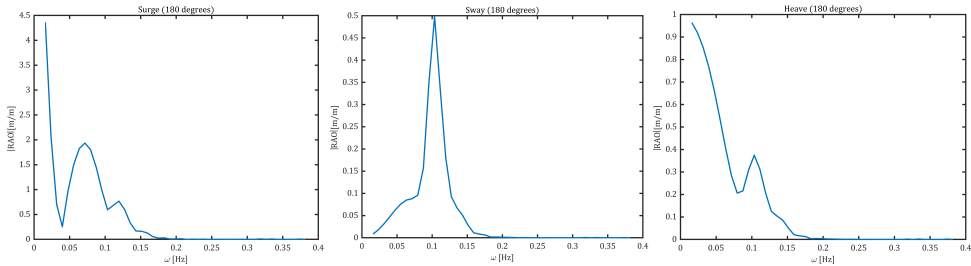


Figure 4.4: Graphical representation of the real parts of the surge, sway and heave RAOs at the crane tip position for an incoming wave direction of 180 degrees.

4.3. TOWER MODEL

To test the feasibility of installing the future generation wind turbines using a floating heavy lift vessel, the response motions of those turbines during installation should be examined in more detail. An overview of state-of-the-art tower structures is presented in Table 4.1. As it might be expected that floating installation is to be used mainly for the installation of large turbines, the 6 and 8 MW towers are chosen to test the feasibility of the concepts. The weight of each tower has been determined using a steel density of 8000 kg/m³.

Table 4.1: Tower dimensions

Capacity [MW]	Supplier	L[m]	D [m]	t [mm]	m [ton]
3	Vestas	69.8	4.48-3.24	20	156
3.3	Vestas	60.0	4.50-3.10	20	135
4	Siemens	76.0	5.50-3.12	16	168
6	GE Hali-ade	100	5.50-4.00	25	344
8	Vestas V164	110	6.50-4.50	17	305

4

During this stage of the research only the phase of the installation just before touchdown of the tower on the transition piece is examined (see Fig. 4.5), since it is expected this will be the most critical case. Assuming a constant crane tip height, the length of the crane wire at the moment just before touchdown will vary for the 6 and 8 MW towers. From this point on a crane wire length of $l_{wr} = 40m$ will be used for the 6 MW tower and $l_{wr} = 30m$ for the 8 MW tower, resembling the case just before touchdown for both towers.

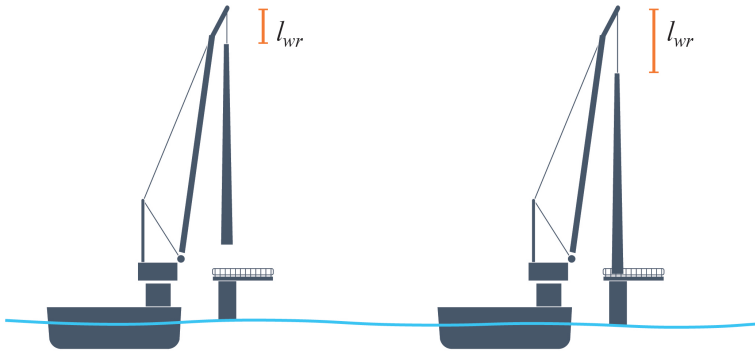


Figure 4.5: Lowering of the tower to the moment just before touchdown [r].

4.3.1. 2D MODEL

According to [DNV, 2011] lifting operations can be classified in two categories depending on the weight of the load and the displacement of the vessel. The two categories are defined as:

- light lifts. The weight of the load is less than 1-2 % of the vessel displacement and is therefore considered small with respect to the vessel weight. In case of light lifts, the load in the crane does not affect the vessel motion.
- heavy lifts. The weight of the load is more than 1-2 % of the vessel displacement and the dynamics of the load in the crane can affect the vessel motion.

Since the weights of the 6 and 8 MW towers are 344 and 305 ton (see Table 4.1) and the vessel displacement is approximately 54000 ton (see Fig. 4.3), the lifting of both towers can be categorized as light lift. As stated above, the vessel motions are not influenced by the load in the crane during light lifts and therefore analysis using motion RAOs will suffice.

To gain a first insight in the response behavior of the tower as a result of the vessel motions, the system is simplified by representing it as a double pendulum with a moving support (Fig. 4.6). The pendulum is composed of two rigid bars. The top one, depicting the crane wire, is assumed to be massless, whereas the bottom one, representing the tower, has a mass equal to the tower mass. The vector $P(t)$ indicates the change in position of the crane tip, due to both horizontal and vertical translations of the tip. Since the response of the vessel, and therefore the response of the crane tip, is assumed to be linear, the response of the double pendulum can also be assumed linear. In this case, the response of the double pendulum can be computed in the frequency domain. Analyzing a system in the frequency domain provides fast and distinct results, which can be used to gain insight into the response of the system.

To compute the response of the tower at the moment just before touchdown, the following steps are followed.

1. Derive equations of motion of the double pendulum
2. Compute the transfer functions $\frac{x_i}{x_{ct}}(\omega)$
3. Compute the transfer functions $\frac{x_i}{\zeta}(\omega)$

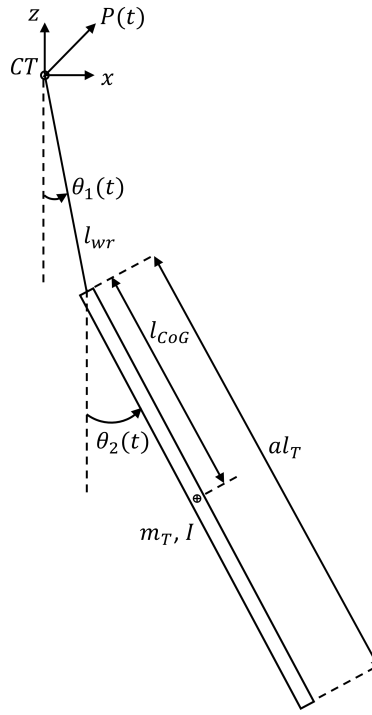


Figure 4.6: Graphical representation of the double pendulum model.

4.3.2. LAGRANGIAN MECHANICS

The equations of motion for the double pendulum can be derived using Lagrangian mechanics. Just as with the virtual work principle, Lagrangian mechanics do not require analysis of all the forces acting on the system, making it a relative fast and easy way to obtain the equations of motion for that system. Another benefit of Lagrangian mechanics is that it allows the user to choose a coordinate system to its liking, thereby introducing the concept of generalized coordinates. Using a generalized coordinate system rather than a conventional coordinate system can ease the analysis of planar motions for example.

For a conservative system, one can use the Euler-Lagrange equations to derive the system's equations of motion. The Euler-Lagrange equations are defined as follows:

$$\frac{d}{dt} \frac{\delta L}{\delta \dot{q}_j} - \frac{\delta L}{\delta q_j} = 0 \quad (4.12)$$

Where q_j and \dot{q}_j are the generalized displacement and velocity for the j^{th} degree of freedom.

The Lagrangian L is defined as:

$$L = T - V \quad (4.13)$$

Where T and V represent the kinetic- and potential energy of the system.

In general, the kinetic energy T and potential energy V of a system can be computed using Eq. 4.14 and Eq. 4.15:

$$T = \frac{1}{2}mv^2 + \frac{1}{2}I\dot{\theta}_0^2 \quad (4.14)$$

$$V = mgz \quad (4.15)$$

4.3.3. DERIVING THE EQUATIONS OF MOTION

To calculate the kinetic- and potential energy one should first define the translations of the point of interest. For this system, the reference point is chosen to be the center of gravity of the tower. The horizontal and vertical position of this point can be written as a function of the crane tip displacement and the angles θ_1 and θ_2 (see Fig. 4.6).

$$\begin{aligned} x_{CoG} &= x_{ct} + l_{wr} \sin \theta_1 + l_{CoG} \sin \theta_2 \\ z_{CoG} &= z_{ct} - l_{wr} \cos \theta_1 - l_{CoG} \cos \theta_2 \end{aligned} \quad (4.16)$$

Differentiating the horizontal- and vertical displacements of the tower C.o.G. gives the velocity of the point in x- and z-direction:

$$\begin{aligned} \dot{x}_{CoG} &= \dot{x}_{ct} + l_{wr} \dot{\theta}_1 \cos \theta_1 + l_{CoG} \dot{\theta}_2 \cos \theta_2 \\ \dot{z}_{CoG} &= \dot{z}_{ct} + l_{wr} \dot{\theta}_1 \sin \theta_1 + l_{CoG} \dot{\theta}_2 \sin \theta_2 \end{aligned} \quad (4.17)$$

The expression for the kinetic energy of the system, as defined in Eq. 4.14, can now be written as:

$$T = \frac{1}{2}m_T(\dot{x}_{CoG}^2 + \dot{z}_{CoG}^2) + \frac{1}{2}I\dot{\theta}_2^2 \quad (4.18)$$

Where the inertia I of the tower is defined as:

$$I = \frac{1}{12}m_T l_T^2 \quad (4.19)$$

Substitution of the vertical displacement z_{CoG} into Eq. 4.15 gives the potential energy required for the Lagrange method.

$$V = m_T g z_{CoG} \quad (4.20)$$

Finally, one can find the Lagrangian by substituting Eq. 4.18 and Eq. 4.20 into Eq. 4.13.

$$L = \frac{1}{2}m_T(\dot{x}_{CoG}^2 + \dot{z}_{CoG}^2) + \frac{1}{2}I\dot{\theta}_2^2 - m_T g z_{CoG} \quad (4.21)$$

At this point, one can derive the equations of motion for the double pendulum system by solving the Euler-Lagrange equations for the generalized coordinates θ_1 and θ_2 . This

results in a system of two coupled equations of motion which, after linearizing for small angles, can be written in matrix form as presented in Eq. 4.22.

$$\begin{bmatrix} m_T l_{wr}^2 & m_T l_{wr} l_{CoG} \\ m_T l_{wr} l_{CoG} & m_T l_{CoG}^2 + I \end{bmatrix} \begin{bmatrix} \ddot{\theta}_1 \\ \ddot{\theta}_2 \end{bmatrix} + \begin{bmatrix} m_T l_{wr} (g + \ddot{z}_{ct}) & 0 \\ 0 & m_T l_{CoG} (g + \ddot{z}_{ct}) \end{bmatrix} \begin{bmatrix} \theta_1 \\ \theta_2 \end{bmatrix} = \begin{bmatrix} -m_T l_{wr} \\ -m_T l_{CoG} \end{bmatrix} \ddot{x}_{ct} \quad (4.22)$$

One might notice that a vertical motion of the crane tip adds a time varying component to the gravitational acceleration. Resulting in a time varying stiffness matrix and a non-linear behavior of the pendulum.

4.3.4. EIGENMODES

A quick analysis into the eigenfrequencies and modes of the system can provide a lot of insight into the behavior of the response of the system. In general, one can calculate the eigenfrequencies for a MDOF system by:

$$\omega_i = \sqrt{\frac{K}{M}} \quad (4.23)$$

Considering Eq. 4.22, the eigenfrequencies for the double pendulum seem to change due to vertical movement of the crane tip. Assuming the vertical acceleration of the crane tip to be small, only the eigenfrequencies and eigenmodes in case $\ddot{z}_{ct} = 0$ are examined. The eigenfrequencies and a graphical representation of the accompanying eigenmodes of the 6 and 8 MW tower in the crane are presented in Fig. 4.7. The first mode describes a slowly swinging motion of the tower about a single rotation point, whereas the second mode shows a higher frequent motion around a node positioned at approximately 60 % of the tower length. Comparing the period of the incoming wave to the eigen period of the system one can estimate the likelihood and potentially prevent the occurrence of resonance.

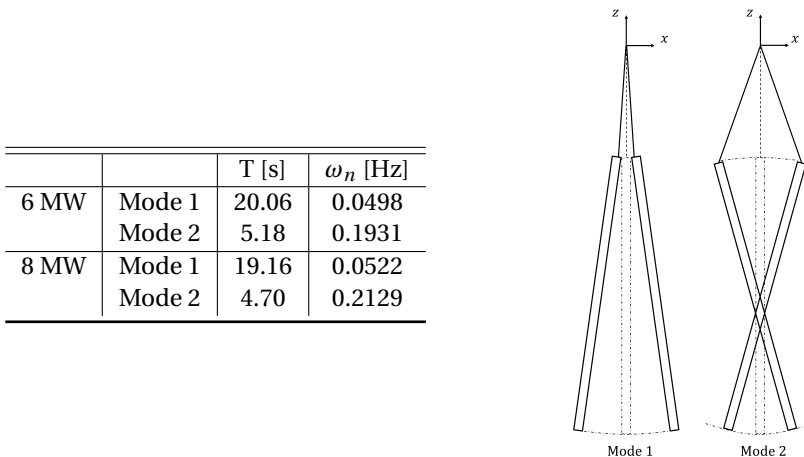


Figure 4.7: Eigenperiods and eigenfrequencies of the system.

4.3.5. MOTION COMPENSATION SYSTEM

The concepts, as presented in Ch. 3, are assumed to be using an actively controlled system, either hydraulic or electrical, to mitigate the response of the tower. The control of an active motion compensation system is software driven, making it possible to design the motion characteristics of the system in an optimal way. To mitigate the tower response, the motion characteristics of the system should consist of two parts:

Part 1: position based. The goal of this part is to keep the position of the gripper constant with respect to the fixed world, thereby mitigating the vessel motions. To do so, the vessel displacements are measured, after which the system's actuators move the system in opposite direction. These characteristics can be represented by a very stiff (virtual) connection between the tower and the fixed world.

Since the tower is not only connected to the vessel through the concept but is also connected to the vessel via the (uncompensated) crane tip, position based compensation might not be enough to control the tower motions since a pure motion compensation system will dissipate almost no energy from the tower motions. To mitigate the tower response, resulting from the displacements of the crane tip, a second characteristic must be added to the software of the system.

Part 2: force based (sky-hook principle). This part can be represented by a (virtual) spring-damper system. The goal of this part is to mitigate the tower motions, induced by the connection between tower and crane tip, with respect to the fixed world.

Since both parts of the motion characteristic are software functions, they can be super positioned and executed simultaneously. Therefore, representing the motion compensation system as a spring-damper connected to the fixed world gives a good representation of a real motion compensation system. This principle can be applied to check if it is possible to control the tower motions to within the limits, specified in Sec. 3.3.

A graphical representation of the model containing the active motion compensation system is presented in Fig. 4.8.

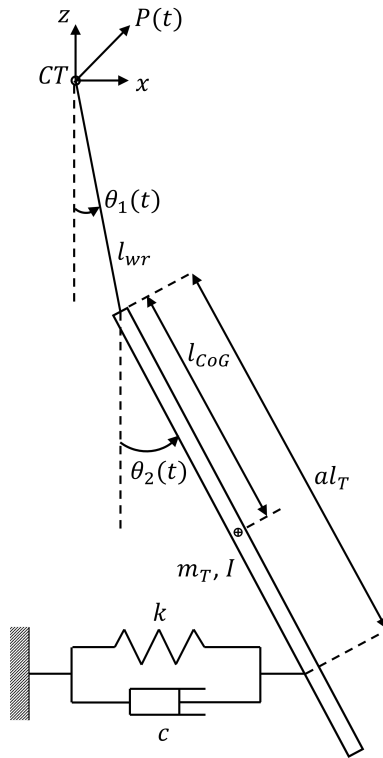


Figure 4.8: Double pendulum model (including spring-damper system)

The EoMs of the system, including the spring-damper, can be obtained in the same manner as explained in Sec. 4.3.3. However, an extra term must be added to the potential energy of the system (Eq. 4.15) to account for the potential energy of the spring. The updated expression for the potential energy of the system is presented in Eq. 4.24.

$$V = m_T g z_{C.o.G.} + \frac{1}{2} k x_s^2 \quad (4.24)$$

Where x_s represents the elongation of the spring as a function of x_{ct} , θ_1 and θ_2 .

$$x_s = x_{ct} + l_{wr} \sin(\theta_1) + a l_T \sin(\theta_2) \quad (4.25)$$

The position of the spring can be varied over the length of the tower by changing the value of the parameter a .

To account for the damping in the system, one should add a dissipative term to the Euler-Lagrange equations from Eq. 4.12. This dissipative term can be expressed in terms of the Rayleigh dissipation function D , given by:

$$D = \frac{1}{2} c \dot{q}_j^2 \quad (4.26)$$

After accounting for the added stiffness and damping in the system, the Euler-Lagrange equations can be written as:

$$\frac{d}{dt} \left(\frac{\delta L}{\delta \dot{q}_j} \right) - \frac{\delta L}{\delta q_j} + \frac{\delta D}{\delta \dot{q}_j} = 0 \quad (4.27)$$

The equations of motion of the double pendulum including the spring-damper system, as presented in Eq. 4.28, can be obtained solving the updated Euler-Lagrange equations for the generalized coordinates θ_1 and θ_2 .

$$\begin{aligned} & \begin{bmatrix} m_T l_{wr}^2 & m_T l_{wr} l_{CoG} \\ m_T l_{wr} l_{CoG} & m_T l_{CoG}^2 + I \end{bmatrix} \begin{bmatrix} \ddot{\theta}_1 \\ \ddot{\theta}_2 \end{bmatrix} + \begin{bmatrix} c l_{wr}^2 & a c l_{wr} l_T \\ a c l_{wr} l_T & a^2 c l_T^2 \end{bmatrix} \begin{bmatrix} \dot{\theta}_1 \\ \dot{\theta}_2 \end{bmatrix} + \dots \\ & \dots + \begin{bmatrix} k l_{wr}^2 + m_T l_{wr} (g + \ddot{z}_{ct}) & a k l_{wr} l_T \\ a k l_{wr} l_T & a^2 k l_T^2 + m_T l_{CoG} (g + \ddot{z}_{ct}) \end{bmatrix} \begin{bmatrix} \theta_1 \\ \theta_2 \end{bmatrix} = \dots \quad (4.28) \\ & \dots - \left(\begin{bmatrix} m_T l_{wr} \\ m_T l_{CoG} \end{bmatrix} \ddot{x}_{ct} + \begin{bmatrix} c l_{wr} \\ a c l_{CoG} \end{bmatrix} \dot{x}_{ct} + \begin{bmatrix} k l_{wr} \\ a k l_{CoG} \end{bmatrix} x_{ct} \right) \end{aligned}$$

4.3.6. TRANSFER FUNCTION DERIVATION

In the following sections of this report the effect of the vertical acceleration of the crane tip (see Eq. 4.28) is ignored, since the vertical acceleration of the crane tip is expected to be small in comparison to the gravitational acceleration. If the vertical acceleration of the crane tip is small compared to the gravitational acceleration, its effect on the tower response is also assumed to be small. However, the effect of ignoring the vertical motion of the crane tip on the response of the tower should be examined in more detail. This is done at the end of this chapter using the static- and dynamic analysis software Orcflex (see Sec. 4.5.2).

By ignoring the vertical motion of the crane tip, linear equations of motion are obtained. Using this property, one can analyze the response of the system in the frequency domain. The response can be computed using transfer functions, which relate a linear output signal to a linear input signal. Assuming that the displacement of the crane tip x_{ct} is a sinusoidal signal, then the first and second derivatives are also sinusoidal functions. Let's assume:

$$\begin{aligned} x_{ct} &= x_{cta} e^{st}, & \theta_i &= \theta_{ia} e^{st} \\ \dot{x}_{ct} &= s x_{cta} e^{st}, & \dot{\theta}_i &= s \theta_{ia} e^{st} \\ \ddot{x}_{ct} &= s^2 x_{cta} e^{st}, & \ddot{\theta}_i &= s^2 \theta_{ia} e^{st} \end{aligned} \quad (4.29)$$

Here, $s = i\omega$. Since, the system is assumed linear the response to a sinusoidal input signal will also be sinusoidal. Substitution of Eq. 4.29 into Eq. 4.28 gives:

$$\begin{aligned}
& \left(s^2 \begin{bmatrix} m_T l_{wr}^2 & m_T l_{wr} l_{CoG} \\ m_T l_{wr} l_{CoG} & m_T l_{CoG}^2 + I \end{bmatrix} + s \begin{bmatrix} c l_{wr}^2 & a c l_{wr} l_T \\ a c l_{wr} l_T & a^2 c l_T^2 \end{bmatrix} + \dots \right. \\
& \dots + \left. \begin{bmatrix} k l_{wr}^2 + m_T g l_{wr} & a k l_{wr} l_T \\ a k l_{wr} l_T & a^2 k l_T^2 + m_T g l_{CoG} \end{bmatrix} \right) \begin{bmatrix} \theta_{1a} \\ \theta_{2a} \end{bmatrix} e^{st} = - \left(s^2 \begin{bmatrix} m_T l_{wr} \\ m_T l_{CoG} \end{bmatrix} + \dots \right. \\
& \dots + s \left. \begin{bmatrix} c l_{wr} \\ a c l_{CoG} \end{bmatrix} + \begin{bmatrix} k l_{wr} \\ a k l_{CoG} \end{bmatrix} \right) x_{cta} e^{st}
\end{aligned} \quad (4.30)$$

One can re-write the above system of equations as two separate equations containing both terms of θ_1 and θ_2 , resulting in Eq. 4.31 and Eq. 4.32.

$$\begin{aligned}
& m_T (l_{wr}^2 \theta_1 + l_{wr} l_{CoG} \theta_2 + l_{wr} x_{ct}) s^2 + c (l_{wr}^2 \theta_1 + a l_{wr} l_T \theta_2 + l_{wr} x_{ct}) s + \dots \\
& \dots + (m_T g l_{wr} + k l_{wr}^2) \theta_1 + k (a l_{wr} l_T \theta_2 + l_{wr} x_{ct}) = 0
\end{aligned} \quad (4.31)$$

$$\begin{aligned}
& (m_T l_{wr} l_{CoG} \theta_1 + (m_T l_{CoG}^2 + I) \theta_2 + m_T l_{CoG} x_{ct}) s^2 + c a l_T (a l_T \theta_2 + l_{wr} \theta_1 + x_{ct}) s + \dots \\
& \dots + a k l_T l_{wr} \theta_1 + a^2 k l_T^2 \theta_2 + a k l_T x_{ct} + m_T g l_{CoG} \theta_2 = 0
\end{aligned} \quad (4.32)$$

Re-arranging Eq. 4.31 to the form $\theta_1 = f(s, \theta_2, x_{ct})$ or $\theta_2 = f(s, \theta_1, x_{ct})$ and substituting the results into Eq. 4.32 gives expressions for θ_1 and θ_2 in terms of s and x_{ct} . Finally, one can derive a transfer function relating the horizontal displacement of the crane tip x_{ct} to the angle of the crane wire θ_1 and the angle of the tower θ_2 with respect to the vertical.

Since the main objective of the motion compensation system is to maintain the horizontal tower motions to within specified limits (Sec. 3.3), it might be interesting to compute the transfer function which relates the horizontal displacement of the crane tip to the horizontal displacement of the top and bottom of the tower. To do so, one should express the horizontal displacement of both the top and bottom as a function of x_{ct} , θ_1 and θ_2 (Eqs. 4.33 - 4.34).

$$x_{top} = x_{ct} + l_{wr} \theta_1 \quad (4.33)$$

$$x_{bot} = x_{ct} + l_{wr} \theta_1 + l_T \theta_2 \quad (4.34)$$

Substitution of θ_1 and θ_2 (as functions of s and x_{ct}) into Eq. 4.33 and Eq. 4.34 results in expressions for x_{top} and x_{bot} depending on s and x_{ct} only. Finally, one can derive the transfer functions relating the horizontal displacement of the crane tip to the horizontal displacement of the tower top and bottom.

In generic form, the complex transfer functions for the horizontal tower top and bottom displacements can be written as:

$$\frac{x_{top}}{x_{ct}} = \frac{n_4 s^4 + n_3 s^3 + n_2 s^2 + n_1 s + n_0}{d_4 s^4 + d_3 s^3 + d_2 s^2 + d_1 s + d_0} \quad (4.35)$$

$$\frac{x_{bot}}{x_{ct}} = \frac{N_4 s^4 + N_3 s^3 + N_2 s^2 + N_1 s + N_0}{d_4 s^4 + d_3 s^3 + d_2 s^2 + d_1 s + d_0} \quad (4.36)$$

Where the numerator terms, denoted by n_i and N_i , are found to be:

$$\begin{aligned} n_4 &= 0 & N_4 &= 0 \\ n_3 &= 0 & N_3 &= 0 \\ n_2 &= m_T^2 g l_{CoG}^2 + m_T g I & N_2 &= m_T^2 g l_{CoG} (l_{CoG} - l_T) + m_T g I \\ n_1 &= m_T g a^2 c l_T^2 & N_1 &= m_T g c l_T^2 a (a - 1) \\ n_0 &= m_T^2 g^2 l_{CoG} + m_T g a^2 k l_T^2 & N_0 &= m_T^2 g^2 l_{CoG} + m_T g k l_T^2 a (a - 1) \end{aligned} \quad (4.37) \quad (4.38)$$

One might notice that the denominator terms in Eq. 4.35 and Eq. 4.36 are the same and are defined as follows:

$$\begin{aligned} d_4 &= m_T l_{wr} I \\ d_3 &= m_T c l_{wr} (a l_T - l_{CoG})^2 + c I l_{wr} \\ d_2 &= m_T k l_{wr} (-a l_T + l_{CoG})^2 + m_T g I \\ d_1 &= m_T g c (a^2 l_T^2 + l_{wr} l_{CoG}) \\ d_0 &= m_T g k (a^2 l_T^2 + l_{wr} l_{CoG}) + m_T^2 g^2 l_{CoG} \end{aligned} \quad (4.39)$$

From Eqs. 4.35 - 4.39 it may be noticed that, assuming the tower-crane configuration does not change, the amplitude of the transfer function depends on the values of s , a , k and c . To illustrate the effect of changing one of these parameters on the response amplitude of the system, a number of situations are examined in more detail.

4.3.7. VALIDATION OF THE TRANSFER FUNCTION

Although the Lagrange method is an effective tool to derive equations of motion, applying the Lagrange method one might lose the physical interpretation of the equations ([Rixen, 2006]). This, together with the lengthy derivation of the transfer functions increases the susceptibility to errors. Therefore, before checking what the effect of changing these parameters on the response of the system will be, it is important to validate the transfer functions themselves. To do so, reference is made to the problem of a simple pendulum on a cart ([González, 2006]), as presented in Fig. 4.9.

The linearized EoM for this simple system is:

$$mL^2\ddot{\theta} + mgL\theta = \ddot{x} \quad (4.40)$$

Where x is the input signal for the cart, which like the crane tip has no mass. The mass m is the point mass at the end of the rigid bar with length L . To compare the response of the double pendulum to the response of the simple pendulum, one should compute the transfer function relating the horizontal displacement of the point mass x_m to the horizontal displacement of the cart x .

Assuming that the input signal describes a sinusoidal motion and the system is linear, the response is also expected to behave sinusoidal and with the same frequency as the input, represented in Eq. 4.41.

$$x = x_a e^{st}, \quad \theta = \theta_a e^{st} \quad (4.41)$$

Then, the transfer function relating the horizontal displacement of the point mass to the horizontal displacement of the cart can be written as:

$$\frac{x_m}{x} = \frac{g/L}{s^2 + g/L} = \frac{\omega_n^2}{s^2 + \omega_n^2} \quad (4.42)$$

If the length of the tower is set to a value $l_T \ll 1$ to approximate a point mass and the length L and the mass m of the simple pendulum are chosen such that they match the length of the crane wire l_{wr} and the mass of the tower m_T , a good comparison between the transfer functions can be made. For small values of l_T , one may assume that the horizontal displacement of the top of the tower x_{top} equals the horizontal displacement of the bottom of the tower x_{bot} . In this situation, the frequency response should be the same (or approximately the same) for both the simple- and double pendulum (see Fig. 4.10).

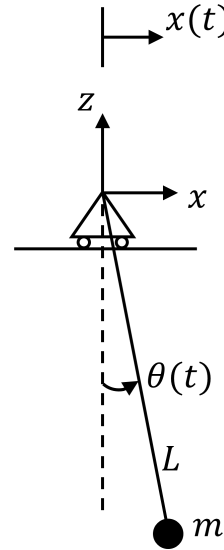


Figure 4.9: Simple pendulum on cart.

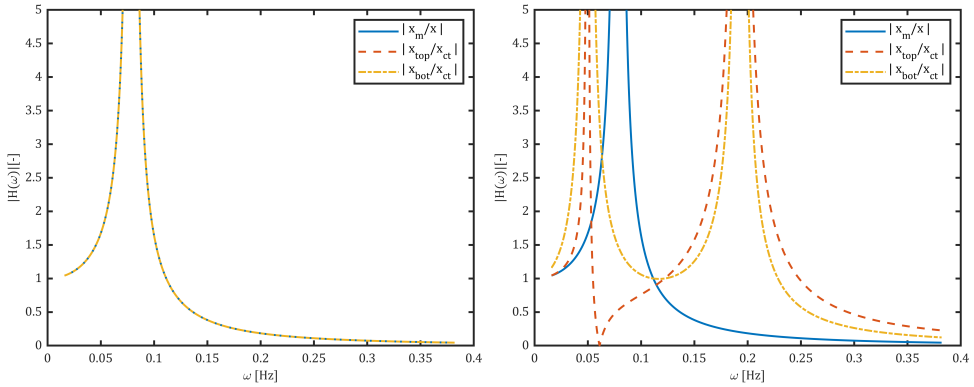


Figure 4.10: Comparing the transfer functions of the simple pendulum on a cart with the double pendulum ($l_T \ll 1$) [l] and the double pendulum ($l_T = 100m$) [r]

The right hand side of Fig. 4.10 shows the real parts of the transfer functions x_m/x , x_{top}/x_{ct} and x_{bot}/x_{ct} for free oscillations of the pendulum (no spring or damper) with a tower length of 100 m. The first thing to note is the presence of two resonance peaks, corresponding with the first and second eigenfrequency of the system (Sec. 4.3.4). Furthermore, one might notice that at a certain frequency the tower top has an anti-resonance. The anti-resonance phenomenon finds its origin in the interference between the two oscillating pendulum parts and can potentially be used to minimize the tower motions.

4.3.8. COUPLING OF TOWER AND VESSEL RESPONSE

Finally, one is interested in the response of the tower in the crane resulting from a change in sea surface elevation. Therefore, one must know how the vessel responds to certain sea-states (Sec. 4.2.4). The complex transfer function relating the horizontal tower displacement to an incoming wave can be computed as:

$$\frac{x_i}{\zeta}(\omega) = \frac{x_{ct}}{\zeta}(\omega) \frac{x_i}{x_{ct}}(\omega) \quad (4.43)$$

Where the transfer function relating the horizontal displacement of the crane tip to the sea surface elevation ($\frac{x_{ct}}{\zeta}(\omega)$) has been derived in Sec. 4.2.5. The transfer functions relating the horizontal tower displacements to the horizontal crane tip displacements ($\frac{x_i}{x_{ct}}(\omega)$) are derived in Sec. 4.3.6.

Using the transfer function, introduced in Eq. 4.43, one can compute the response of the tower to an incoming wave. One can vary the parameters a , k and c to, ultimately, minimize the response function. Arbitrary stiffness ($k = 1e3kN/m$) and damping ($c = 1e2kNs/m$) values are used to calculate the tower response with respect to incoming waves. Fig. 4.11 - Fig. 4.12 show the response of the top and bottom of the tower for various positions of the motion compensation system along the tower height. As stated in the design requirements from Sec. 3.3, the wave periods of interest lie in the range

between 6 - 9 s. The range of wave periods is indicated in Fig. 4.11 - 4.12 by the blue frequency band.

One may conclude that varying the position of the spring-damper system along the height of the tower affects the extent to which the tower responds on the incoming waves. It can be noted that by gradually shifting the position of the spring-damper system from the top of the tower to the bottom of the tower, the position of the resonance peak shifts in the frequency domain. By changing the parameters a , k and c , the system's stiffness matrix changes, resulting in new eigenfrequencies. In theory, one could vary the parameters in such a way that no resonance peaks occur in or in proximity of the interesting wave frequencies.

4

Considering the transfer functions presented in both figures more closely, some interesting results can be derived.

- Positioning the motion compensation system at the top of the tower ($a=0$) results in small responses of the top and bottom of the tower in the frequency range of interest.
- Positioning the motion compensation system at the bottom of the tower ($a=1$), the system has an eigenfrequency in the frequency range of interest. This can result in large tower motions.

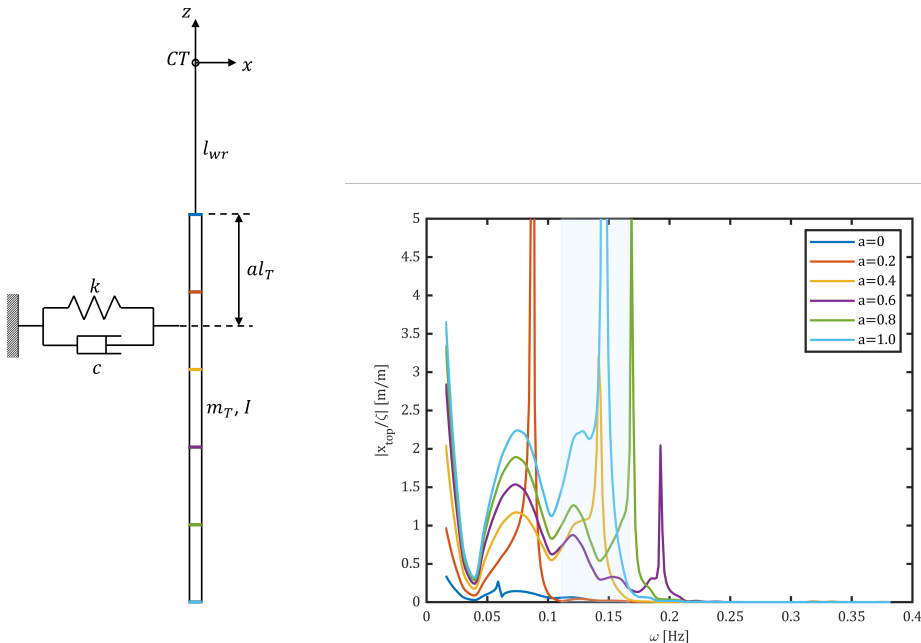


Figure 4.11: Transfer function relating the horizontal top displacement of the tower to the sea surface elevation for a varying position of the motion compensation system [1], $k = 1000kN/m$ and $c = 100kNs/m$.

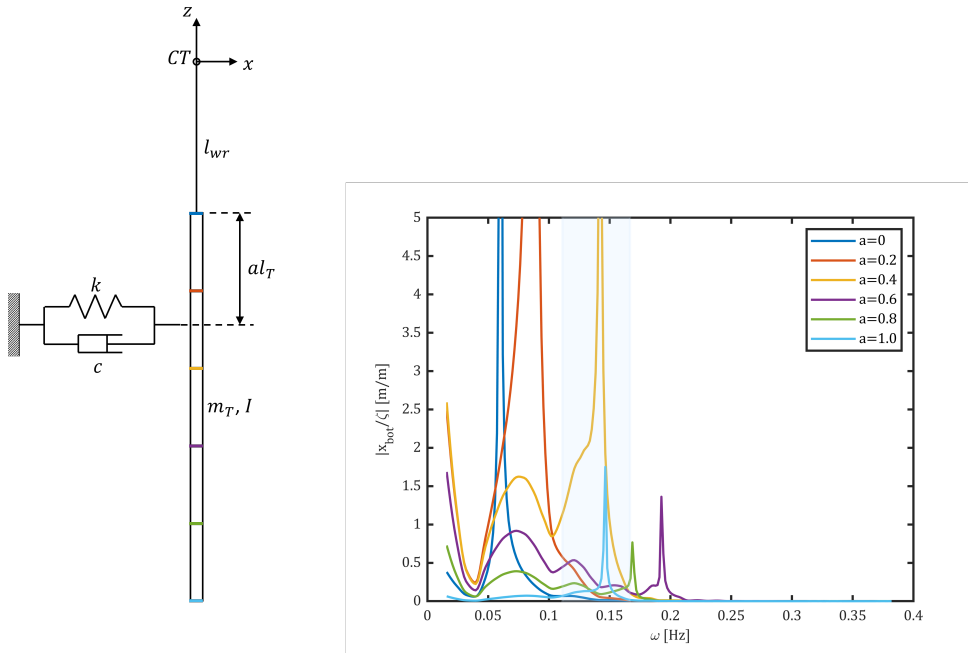


Figure 4.12: Transfer function relating the horizontal bottom displacement of the tower to the sea surface elevation for a varying position of the motion compensation system, $k = 1000 \text{ kN/m}$ and $c = 100 \text{ kNs/m}$.

4.4. OPTIMIZATION

From the previous section, one can conclude the following:

- retaining the motions at the top of the tower is an effective way to mitigate the bottom displacement of the tower
- retaining the motions at the bottom of the tower can result in large displacements of the top of the tower

Its likely good solutions, resulting in low responses, exist for $0 < a < 1$ in the specified wave frequency range. These solutions can be found by changing the values of a , k and c to minimize the tower response. However, as stated before, low response at one point of the tower could possibly coincide with large response at another point.

To account for the shape and size of the (resonance) peaks in the transfer functions, one should analyze the response spectra rather than the transfer functions. As both the displacement of the top and bottom are of importance for safe installation of the tower, a combination of the two should be optimized. To do so, a cost function C is introduced covering the horizontal motion of both the top and bottom in terms of the significant response amplitude (see Eq. 4.44). The displacement of the bottom of the tower is assumed to be the governing factor during installation, therefore it has been assigned a

bigger weight on the cost function.

$$\mathbf{C}(a, k, c) = \frac{\bar{x}_{top1/3} + 2\bar{x}_{bot1/3}}{3} \quad (4.44)$$

The significant response amplitude equals two times the Root Mean Square value of the response spectrum (Eq. 4.45).

4

$$\bar{x}_{i1/3} = 2RMS = 2\sqrt{m_{0,x}} \quad (4.45)$$

Finally, the combination of a , k and c for which the cost function has its absolute minimum is to be found (see Eq. 4.46).

$$\text{Min}\{\mathbf{C}(a, k, c)\} = \text{Min}\left\{\frac{\bar{x}_{top1/3} + 2\bar{x}_{bot1/3}}{3}\right\} \quad (4.46)$$

To do so, Matlab's *fminsearch* function is used in combination with upper and lower limit boundaries for a , k and c . It has become clear from Sec. 4.3.8 that restraining the tower motions at the top of the tower is an effective, but potentially expensive, way of mitigating the bottom displacements. As this option basically resembles the motion compensated crane it is not desired as optimal solution. To prevent this option from showing up as the optimal configuration during the optimization process, it is not considered in the optimization process.

During the installation process the tower will be lifted from deck, positioned above the TP and finally be lowered on the TP. To check the effect of varying the crane wire length, due to lifting and lowering of the tower, on the optimal position of the motion compensation system the optimization process has been repeated for multiple crane wire lengths. Apart from varying the length of the crane wire, the influence of the design environmental conditions on the cost function has also been examined. The results of the analyses are presented in Fig. 4.13.

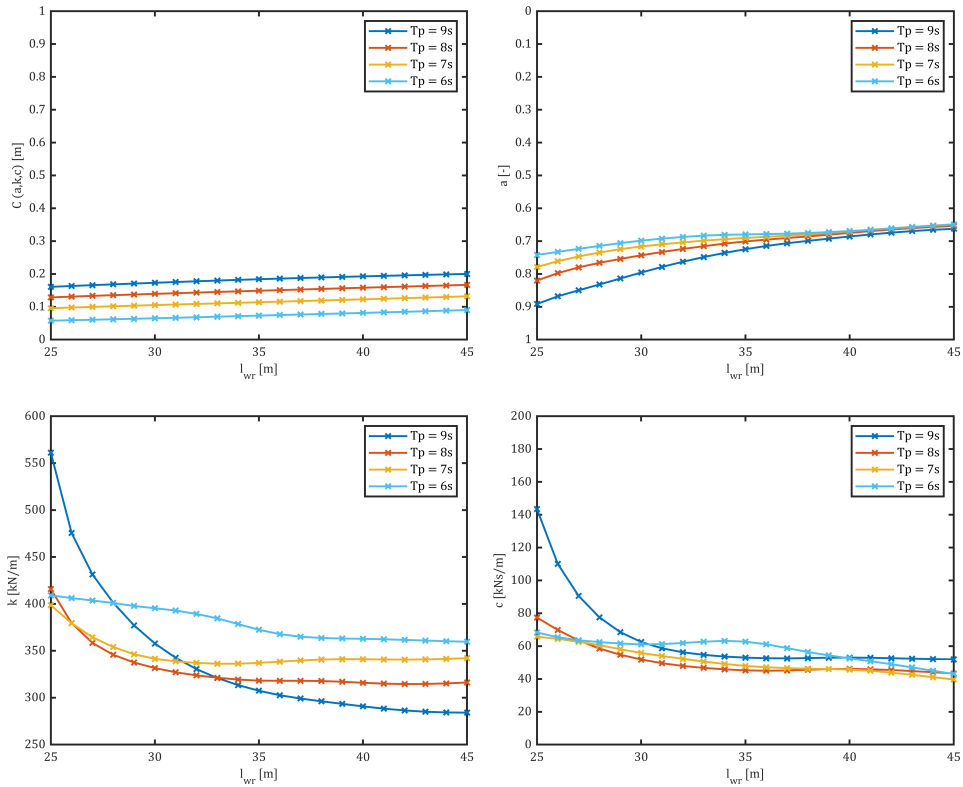


Figure 4.13: Influence of lifting and lowering the tower on the optimized value of the cost function and the corresponding values of a , k and c .

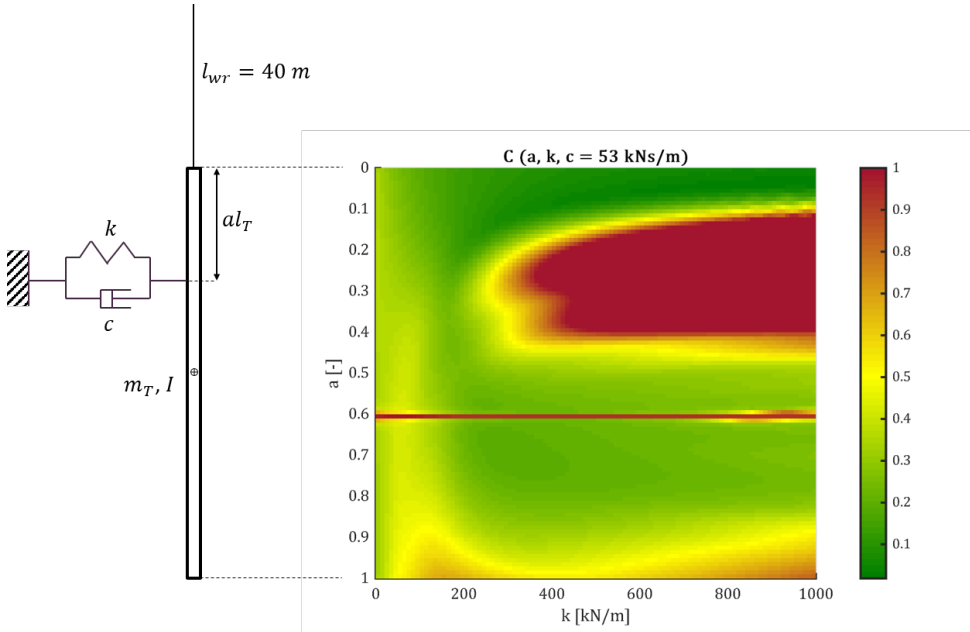
From Fig. 4.13 it becomes clear the value of the cost function and as such, the magnitude of the response motions, increases with an increasing crane wire length (lowering of the tower). Additional, and out of design considerations, meaningful results are the change in optimal position of the motion compensation system along the tower height and the decreasing values of k and c accompanying an increase in crane wire length. When using hydraulic cylinders, the values of stiffness and damping can easily be changed in the software to maintain the optimal value during lifting and lowering.

Similar trends, like in Fig. 4.13, have been obtained for the 8 MW tower. Therefore, as expected, the moment just before touchdown is the most critical for both towers, since at touchdown the length of the cranewire is the longest. The optimal configuration of the motion compensation system for both towers at the moment just before touchdown is presented in Table 4.2.

Table 4.2: Optimal compensating configurations for both towers.

	l_{wr} [m]	a [-]	k [kN/m]	c [kNs/m]
6 MW	40	0.69	291	53
8 MW	30	0.81	319	60

To represent the influence of changing the optimal configuration of a , k and c for the 6 MW tower, the cost function has been calculated for two specific cases. The first case being the situation just before touchdown of the tower on the transition piece and the second case being the situation of the tower lifted up high. Fig. 4.14 shows results of the cost function C for various values of a and k , a constant $c = 53 \text{ kNs/m}$ and a crane wire length $l_{wr} = 40 \text{ m}$. To represent the second case, the cost function has been computed for the same set of parameters a , k and c but with a crane wire length $l_{wr} = 25 \text{ m}$ (see Fig. 4.15).

Figure 4.14: Values of the costfunction of the 6 MW tower for various a and k , $c = 53 \text{ kNs/m}$ and $l_{wr} = 40 \text{ m}$.

From Fig. 4.14 it can be noticed that large responses are to be expected for $0.1 < a < 0.4$ in combination with high stiffness values. On top of that, large responses are likely to occur for $a = 0.6$ and $0.9 < a < 1$. To fully understand why these large responses occur, a closer look must be taken at the frequency response of both the double pendulum and the vessel.

For $0.1 < a < 0.4$, it turns out that the vessel pitch eigen frequency coincides with the eigen frequency of the tower, which also seems to coincide with the peak period of the wave spectrum. For $a = 0.6$, the spring-damper is positioned directly in a node of the second eigenmode resulting in no (or very little) compression/elongation of the spring-damper. When $0.9 < a < 1$, the displacements at the top of the tower become relatively large (as discussed in Sec. 4.3.7).

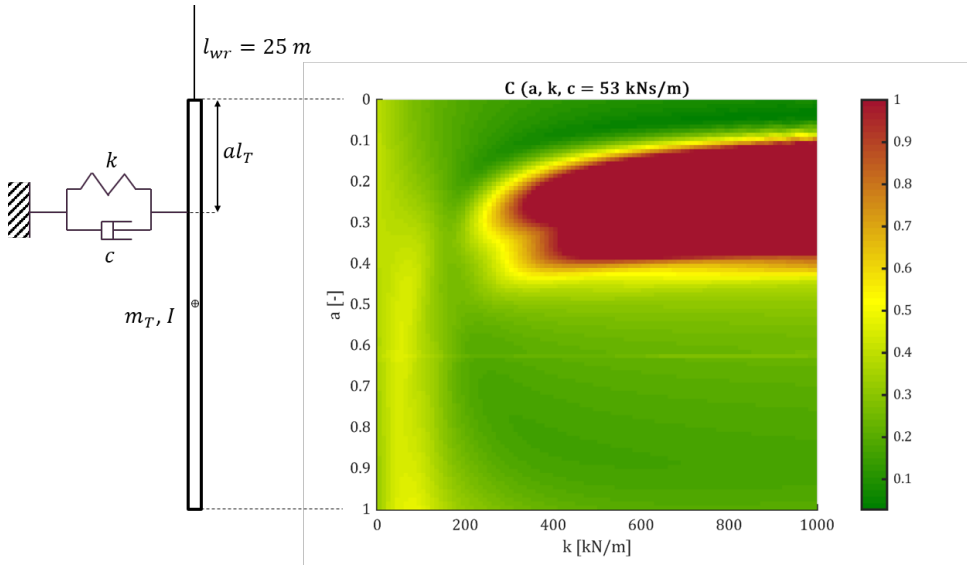


Figure 4.15: Values of the costfunction of the 6 MW tower for various a and k , $c = 53 \text{ kNs/m}$ and $l_{wr} = 25 \text{ m}$.

Comparing the results of Fig. 4.14 and Fig. 4.15, one might conclude that even for a shorter crane wire length, large responses are expected when the compensation system is positioned in the range $0.1 < a < 0.4$.

4.5. ORCAFLEX

In Sec. 4.3.6 the vertical motion of the crane tip has been ignored to obtain linear equations of motion and as such, be able to analyze the response of the system in the frequency domain using transfer functions. To justify the decision, the assumption is made that the influence of the vertical acceleration of the crane tip is small in comparison to the gravitational acceleration and therefore, ignoring the vertical acceleration of the crane tip will still yield a good approximation of the tower response.

In this section Orcaflex is used to check the effect of ignoring the vertical acceleration on the response of the tower. Orcaflex is also used to validate the transfer functions for the optimal configurations of the compensating system for the 6 and 8 MW towers at the moment just before touchdown on the TP, as found in the preceding section, and to analyze the response of the tower in the time domain. To do so, a model has been created following the considerations below.

4

4.5.1. MODEL

Orcaflex is a software package often used by companies in the maritime- and offshore industry to perform dynamic analyses of marine systems, such as analysis of mooring systems and lifting operations. The software package can be used to perform analyses in both frequency- and time domain. A great benefit of using Orcaflex is the graphical 3D representation of the results which allows the user to perform an easy sanity check of the results.

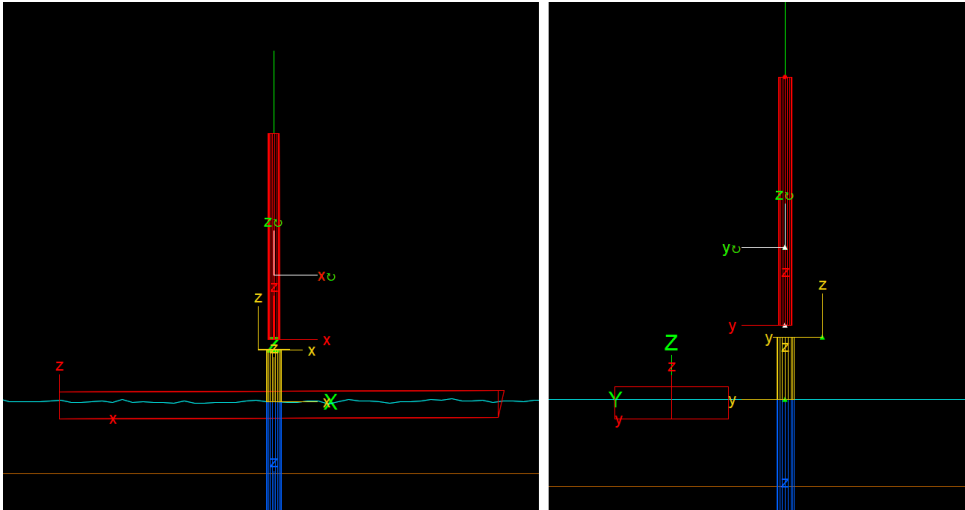


Figure 4.16: Orcaflex model.

The model constructed to check the results from Matlab is a fairly simple model (see Fig. 4.16). The model set-up is discussed in more detail below.

MOTIONRAOs

According to DNV (Sec. 4.3.8), the dynamics of the tower in the crane do not influence the vessel motions and therefore the use of motion RAOs will suffice to analyze the response of the system. The benefits of using motion RAOs instead of load RAOs is that it reduces the simulation time and complexity of the model.

By using motion RAOs and linearization of the system, the effect of potential second order effects are excluded from the results. However, the dynamic response of the tower will be governed by the first order vessel motions, since the frequency range of the first order vessel motions is close to, or coincides with, the natural frequencies of the tower. Second order vessel motions originating from wave drift forces and dynamic positioning are typically in a much lower frequency range and are therefore not assumed to be limiting for the operation.

ENVIRONMENTAL CONDITIONS

The wave conditions in which the system should be able to safely install tower structures are defined in the Functional Requirements (Sec. 3.3) to be $H_s = 2.5m$ and $T_p = 6 - 9s$. From the study into the effect of the wave period on the response of the system (Sec. 4.4) one can conclude that the largest responses are expected for a peak period of 9s. Therefore, the wave conditions for the Orcaflex simulations are chosen to be $H_s = 2.5m$, $T_p = 9s$, where a JONSWAP spectrum is used to generate the sea-states for the simulation.

WAVE HEADING: 180 DEGREES

The analyzed wave heading is chosen to be 180 degrees as it is most likely the crew of a vessel will choose this heading during installation.

TOWER: RIGID BODY

The tower is modelled as a rigid body. The choice has been made to model the tower as a rigid body for two reasons:

1. Easy comparable with the Matlab model
2. Reduces the simulation time significantly

CRANE WIRE

To construct the Matlab model the crane wire has been modelled as a massless rigid body, whereas in reality the crane wire should have a mass and stiffness. Although the mass of the crane wire is negligible, real stiffness values are used for the Orcaflex model. The crane wire stiffness depends on the Young's modulus of the crane wire material (E), the cross sectional area of the crane wire (A), the number of hoisting ropes (n) and the length of the wire (l_{wr}) as given by Eq. 4.47.

$$k_{wr} = \frac{EA_{wr}n}{l_{wr}} \quad (4.47)$$

For the simulation vessel used, the crane wire parameters are: $E = 1.11e5N/mm^2$, $A_{wr} = 1.57e3mm^2$ and $n = 24$.

COMPENSATION SYSTEM: CONSTRAINT FUNCTION

The spring-damper system is modeled using the Orcaflex constraint function. Constraints can be denied motion in specific DoFs. This function can be used to exclude the response of the system in a certain direction. Furthermore, one can assign a stiffness and damping value to a constraint. By doing so, one can represent the simple Matlab model in Orcaflex. Eventually, extra DoFs can be added to check their effect on the response of the tower.

FREQUENCY DOMAIN ANALYSIS

Solving dynamic problems in the frequency domain is a convenient method of analyzing the response of a system, since, as opposed to a time domain solve, the response of the system can be computed over the entire wave frequency range using transfer functions. Whereas in the time domain the wave spectrum is used to generate a certain sea state, as discussed in Sec. 5.4.4 of [Journée et al., 2015]. A downside of the frequency domain method is that it requires systems to be linearized.

TIME DOMAIN ANALYSIS

As mentioned before, time domain simulation requires a time history of the sea surface elevation on a specific time interval. As obtaining (and using) measured data might be troublesome, one can create a time trace of the sea surface elevation using a wave spectrum and choose the spectral parameters in such a way that it resembles the desired sea state. A re-occurring problem when analyzing dynamic systems in time domain is the question what simulation time should be used for the simulation, such that one encounters the extreme response of the system.

SPECTRAL RESPONSE ANALYSIS

To check the effect of linearization on the response of the system, the (not linearized) response characteristics are calculated using Orcaflex's spectral response analysis. The spectral response analysis subtracts a transfer function using the results of a random wave time domain simulation by applying the Fast Fourier Transform. The wave spectrum is represented by a white noise spectrum with the same energy as the JONSWAP spectrum with a significant wave height of $H_s = 2.5m$. In contrast to a normal wave spectrum, the wave energy is distributed equally over the frequency interval. As time domain simulation does not necessarily require a system to be linear, the effect of linearization on the response of the system can be checked.

SIMULATION TIME

In engineering practice, it is often assumed the probability an extreme wave occurs equals $1/1000$. So, if one sets the simulation time equal to the time it takes for 1000 waves to pass the vessel, in theory, an extreme wave should be observed. As for this research the interest lies in the response of the tower in the crane, the simulation time is based on 1000 times the longest natural period of a free hanging tower. The free hanging tower is taken as a reference, because here the biggest responses are expected. Although not necessary, the same simulation time has been chosen for each simulation. For a crane wire length of 40 m, the longest eigen period of the system is 20.06 s and therefore the simulation time is approximately 20100s.

4.5.2. VALIDATING THE TRANSFER FUNCTIONS

In this section the optimal configurations for the motion compensation system, as presented in Sec. 4.4, are used in Orcaflex to compute transfer functions relating the horizontal top and bottom displacement of the tower to a change in the sea surface elevation. Different simulation methods are used to determine the transfer functions with Orcaflex, which can be used to check the transfer functions presented earlier in this chapter.

To derive the transfer functions that relate the horizontal displacements of the tower top and bottom to the sea surface elevation, the system has been simplified (Sec. 4.3.6). An overview of the main simplifications is listed below.

- Small angles were assumed, thereby linearizing the system.
- The pendulum parts are represented as rigid rods, whereas in reality both will have a stiffness and inertia.
- The vertical motion of the crane tip is set to zero, to eliminate non-linear effects induced by the vertical acceleration of the crane tip.

To examine the effect of these simplifications, the Matlab model is validated using Orcaflex. To do so, the transfer functions for the horizontal tower displacements are computed using both Orcaflex's frequency domain (FD) and spectral response analysis (SA) simulation methods. Since FD analysis requires linearization of the system, it is expected that the results obtained with this method will match the transfer functions from the Matlab model. The SA method is based on a time domain simulation, therefore the effect of any non-linearities should be visible in the transfer function computed with this method. An overview of the transfer functions, obtained with each method, is presented in Fig. 4.17 and Fig. 4.18.

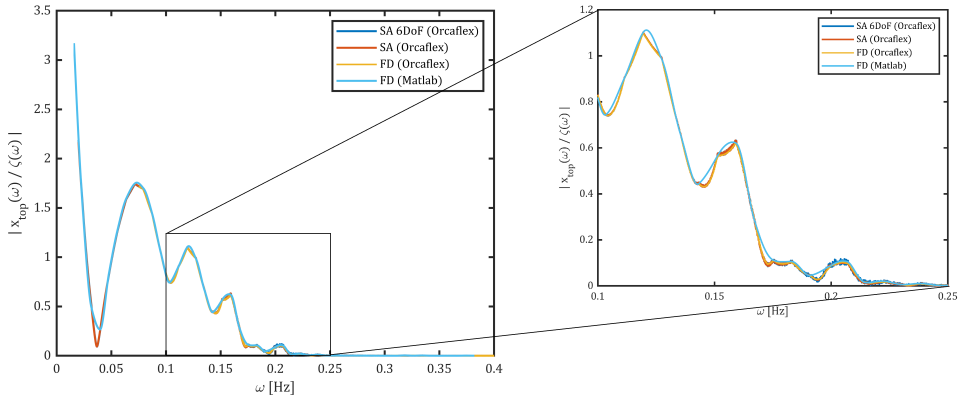


Figure 4.17: Comparison of the TFs x_{top}/ζ obtained using multiple simulation methods (6 MW tower).

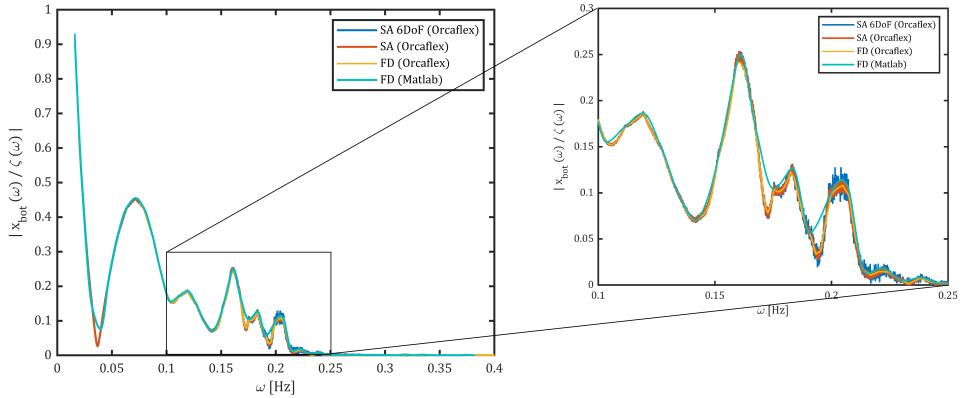


Figure 4.18: Comparison of the TFs x_{bot}/ζ obtained using multiple simulation methods (6 MW tower).

To compute the SA and FD transfer functions, the vessel's sway, heave and roll RAOs have been set to zero, such that primarily horizontal motions of the crane tip are considered. The SA 6DoF graph is constructed resulting from the vessel moving in all directions. From Fig. 4.17 and Fig. 4.18 it can be noticed that the transfer functions obtained with the three methods (SA, FD and Matlab) show great similarities in shape. Looking at the close-up representations of the graphs, it becomes clear that the transfer functions obtained with Matlab are less detailed and show a much smoother behavior than the ones obtained with Orcaflex. This could partially be explained by the fact that the Matlab model assumes the crane wire to be rigid, whereas a 'real' crane wire stiffness has been used for the Orcaflex simulations. An additional factor causing the difference between the transfer functions obtained with Matlab and Orcaflex could be the frequency step size used to compute the transfer functions. Finally, after closer examination of the transfer functions one can conclude the SA methods gives noisy results (especially in the high frequency intervals). Since the effect of the vertical crane tip motion as a result of

the vessel heave is expected to be small for high wave frequencies, the noisy behavior will rather be the result of errors in the conversion of the results from time to frequency domain.

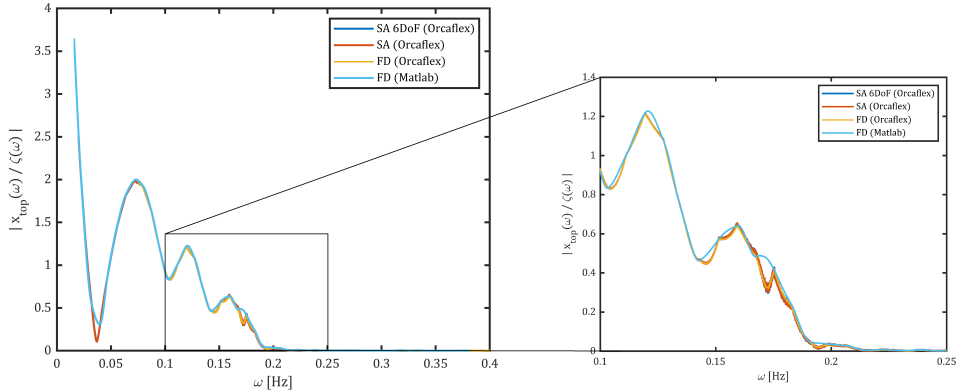


Figure 4.19: Comparison of the TFs x_{top}/ζ obtained using multiple simulation methods (8 MW tower).

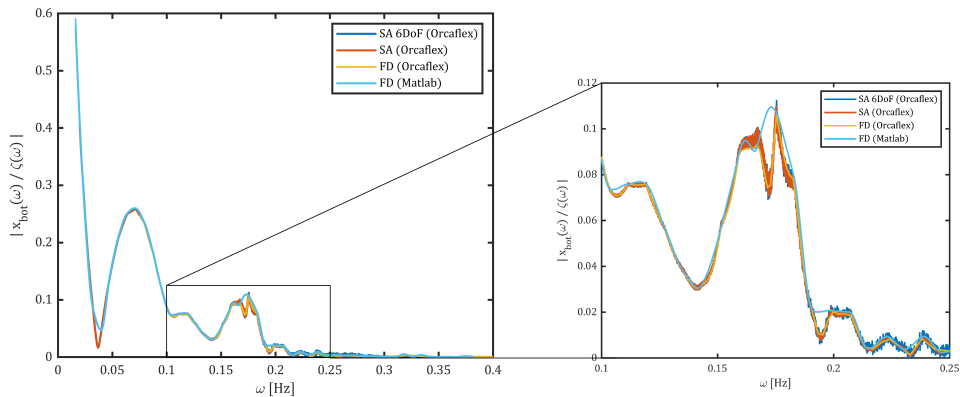


Figure 4.20: Comparison of the TFs x_{bot}/ζ obtained using multiple simulation methods (8 MW tower).

The results presented in Fig. 4.19 and Fig. 4.20 show similar trends to the results from Fig. 4.17 and Fig. 4.18. However, the response of the tower to incoming waves is different in both cases. Comparing the transfer functions of the 6 and 8 MW towers, one may conclude that the response for the bottom of the 8 MW tower is lower than for the 6 MW tower. As the length of the crane wire for the 8 MW tower is shorter than for the 6 MW tower this follows the trend noticed in Sec. 4.4.

Although the transfer functions, presented in Fig. 4.17 – 4.20 can be used to compare the linear and non-linear response of the tower to a change in sea surface elevation over the

entire frequency range, one might be more interested to which account the response of the tower to a specific sea state is affected by non-linear effects. To compare the response of the tower to a specific sea state obtained using the multiple transfer functions, one can compute the standard deviation of the response, which equals the RMS value of the response spectrum (see Eq. 4.48). A JONSWAP spectrum has been used to represent a sea state with a significant wave height $H_s = 2.5m$ and a peak period $T_p = 9s$. The results for both the 6 and 8 MW tower are presented in Table 4.3 and Table 4.4 respectively.

$$\sigma = \sqrt{\int_{\omega_1}^{\omega_2} \left| \frac{x_i}{\zeta}(\omega) \right|^2 S_{wave}(\omega) d\omega} \quad (4.48)$$

Where x_i is used to indicate both the top and bottom displacements of the tower.

Table 4.3: Standard deviations of the response of the 6 MW tower for the different frequency domain methods.

	SA 6DoF	SA	FD	FD (Matlab)
x_{top} [m]	0.50	0.50	0.50	0.51
x_{bot} [m]	0.11	0.11	0.11	0.11

Table 4.4: Standard deviations of the response of the 8 MW tower for the different frequency domain methods.

	SA 6DoF	SA	FD	FD (Matlab)
x_{top} [m]	0.56	0.56	0.56	0.57
x_{bot} [m]	0.05	0.05	0.05	0.05

Comparing the standard deviations obtained using the different transfer functions, one can conclude that the effect of any non-linearity's on the response of the tower are negligible for the chosen sea state. Although the Matlab and Orcaflex transfer functions do show some differences, the standard deviations between the different methods are more or less similar. An explanation for this can be that the wave spectrum used to obtain the standard deviations has a peak period of 9s. This corresponds to a wave frequency $\omega = 0.11Hz$ at which point all transfer functions are matching. A difference between Matlab and Orcaflex might be noticed when choosing a wave spectrum with a peak period of 6s. However, as the linear and non-linear transfer functions computed with Orcaflex do match with each other over the entire frequency range, the effect of any non-linearity's on the response of the tower is still expected to be negligible.

4.5.3. TIME DOMAIN SIMULATION

Although transfer functions provide very useful insight into the response behavior of the system, time domain simulations can be used to check and simulate the effect of nonlinearities. This section covers results of the time domain simulation for both the 6 and 8 MW towers. As discussed in Sec. 4.5.1, the simulation time is chosen to be 20100 s. The results from the time domain simulations are used to check for extreme responses and if the displacement of the bottom exceeds the limits specified in Sec. 3.3. Two different cases, as presented in Fig. 4.21, are examined in the time domain. In the first configuration, the response of the free hanging tower is computed. In the second case, the motions of the tower are examined when motion compensation is applied in both x- and y-direction. It should be noted that, till now, only the response of the tower in the x-direction has been examined. This is done, because in head waves this is the most governing (and normally the only) direction. However, due to a misalignment of the vessel C.o.G. the vessel is also subjected to a small roll motion. This will affect the tower response and, as a result, a circular movement of the tower is expected.

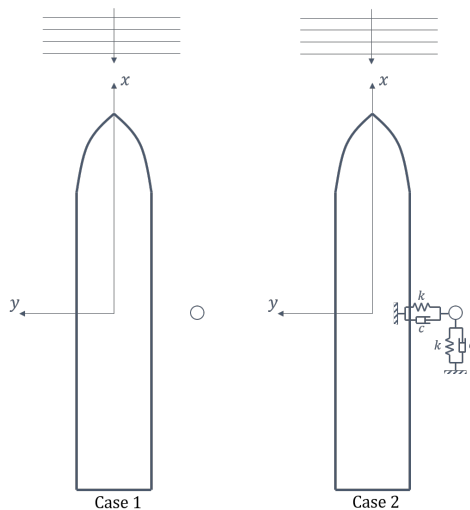


Figure 4.21: Orcaflex time domain configurations: free hanging tower [l], compensated tower [r].

Before discussing the time domain results for the tower including the motion compensation system, the responses of the crane tip and the free hanging tower are examined. The translations of the crane tip, as presented in Fig. 4.22, are computed with respect to the initial position of the crane tip (see Fig. 4.1). As expected, the magnitude of the crane tip surge motion is much bigger than its sway- and heave translations, since for an incoming wave direction of 180 degrees the vessel's pitch motion is governing the response.

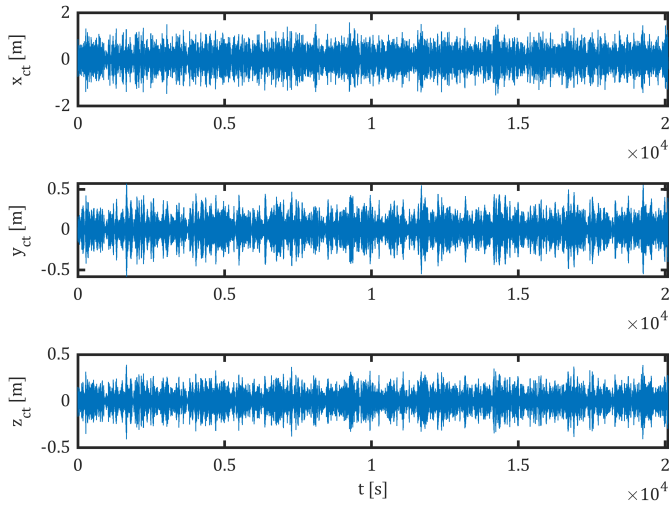


Figure 4.22: Translations of the crane tip.

CASE 1: FREE HANGING TOWER

The response of the free hanging tower to a sinusoidal input signal has been discussed in Sec. 4.3.7. The response of the system without stiffness or damping can become quite severe when the frequency of the input signal coincides with the eigen frequencies of the system. In reality, the system will always be exposed to some stiffness and damping, therefore expecting such extreme motions will be too conservative. To gain some insight in the magnitude of the response of the free hanging tower to incoming waves, the translations of the tower top and bottom are presented for the 6 MW tower in Fig. 4.23 and Fig. 4.24 and for the 8 MW tower in Fig. 4.25 and Fig. 4.26.

As stated in the Functional Requirements (Sec. 3.3) the horizontal displacements of the tower bottom, still ensuring safe installation, are allowed a motion with a most probable maximum of $0.2m$ in both x - and y -direction, whereas the allowable limit for the vertical displacements of the bottom is set to a most probable maximum of $0.1m$. The limits are indicated in Fig. 4.24 and Fig. 4.26 using the red lines.

To test if the tower displacements fulfill the requirement for safe installation in the simulated time interval, the most probable maximum has been computed for each time series. To determine the value of the most probable maximum, reference is made to Sec. 5.3.4.5 in [Journée et al., 2015], where, assuming the response to be Rayleigh distributed, the most probable maximum is defined as:

$$x_{max} = 1.86\bar{x}_{1/3} = 1.86(2\sigma) \quad (4.49)$$

The most probable extremes for each time series are indicated by a green line in Fig. 4.24 and Fig. 4.26. From the figures, one may conclude that the computed most probable extremes are situated outside the limits and therefore, it is not safe to install towers in the

free hanging condition.

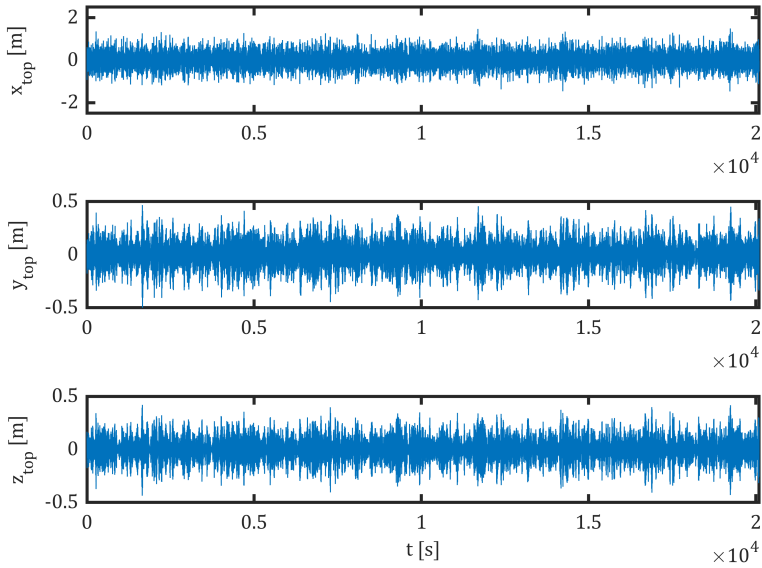


Figure 4.23: Free translations of the top of the 6MW tower.

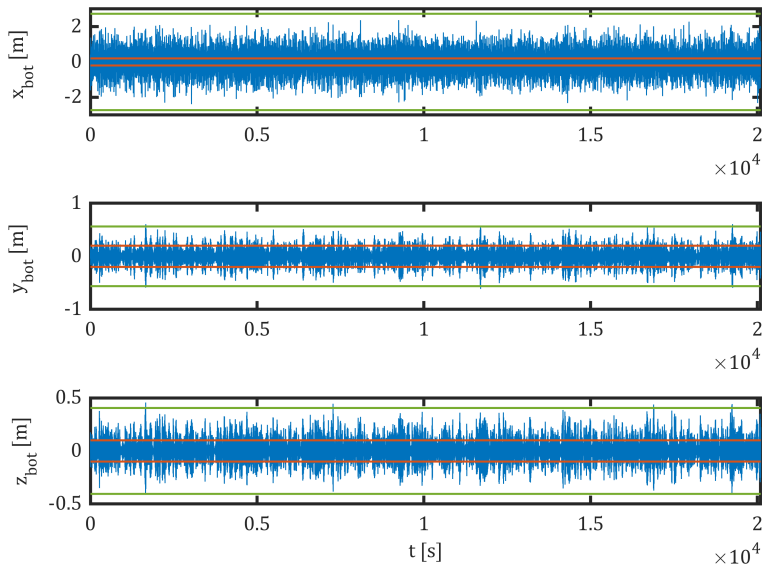


Figure 4.24: Free translations of the bottom of the 6MW tower.

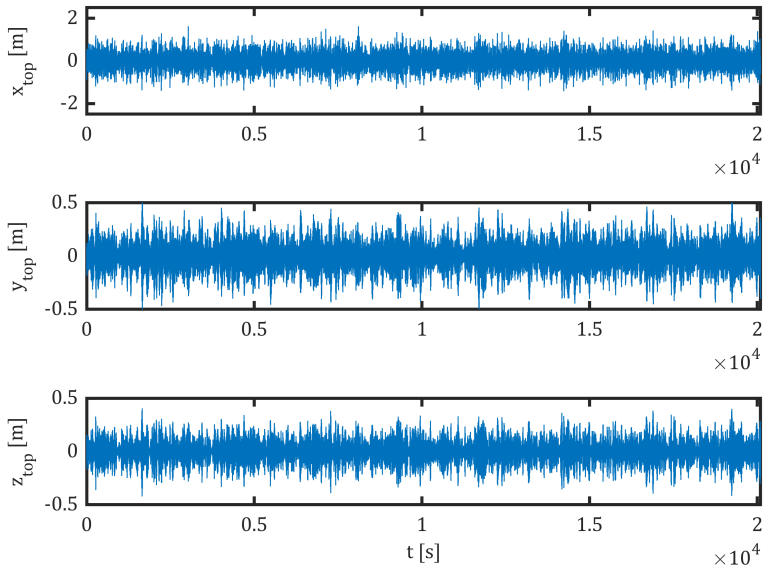


Figure 4.25: Free translations of the top of the 8MW tower.

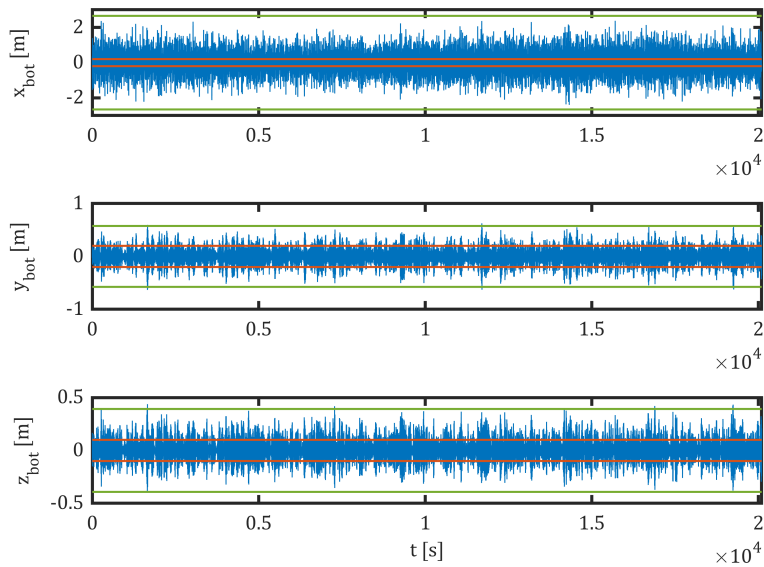


Figure 4.26: Free translations of the bottom of the 8MW tower.

CASE 2: 6 MW TOWER

Considering the results from Case 1, the need for a motion compensation system to control the tower motions can be justified. The first case to be tested, including motion compensation, is the response of the 6 MW tower in the crane. The results are obtained using a crane wire length $l_{wr} = 40\text{m}$ and the corresponding optimal values for $a = 0.69$, $k = 291\text{kN/m}$ and $c = 53\text{kNs/m}$. These parameters represent the condition just before touchdown of the tower.

Comparing the results of the free hanging tower (Fig. 4.23 and Fig. 4.24) with the results of the restrained tower (Fig. 4.27 and Fig. 4.28), one can conclude that the surge and sway response of the tower top has increased slightly. However, the magnitude of the tower bottom surge has seen a significant decrease. The response of the tower resulting y-direction has also been reduced significantly and fulfills the requirements stated in Sec. 3.3.

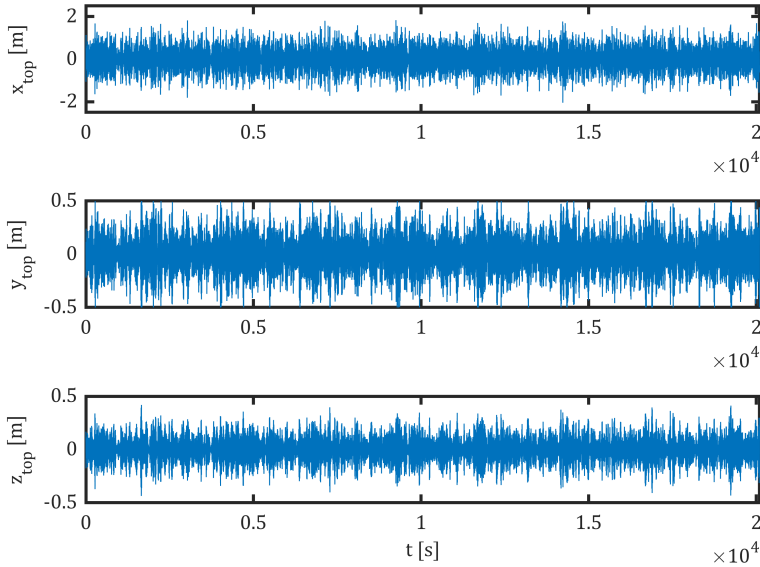


Figure 4.27: Translations of the top of the 6MW tower for $a = 0.69$, $k = 291\text{kN/m}$, $c = 53\text{kNs/m}$. Motion compensation applied in x- and y-direction.

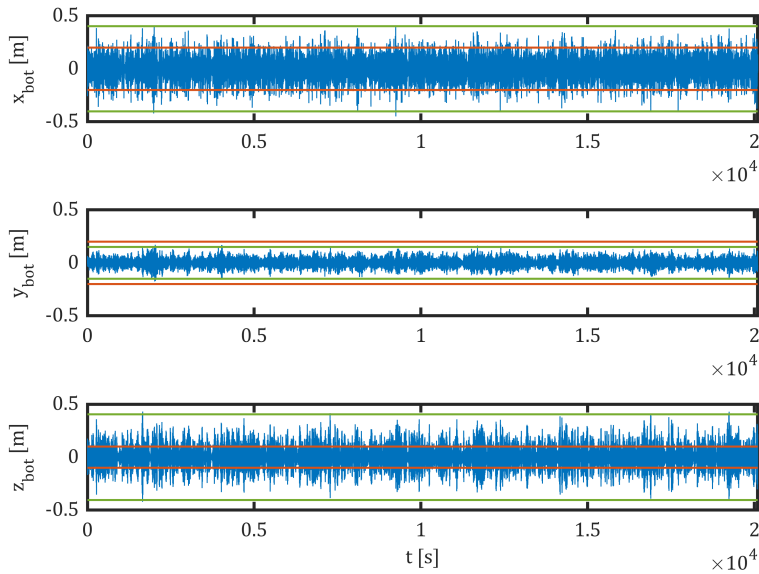


Figure 4.28: Translations of the bottom of the 6MW tower for $a = 0.69$, $k = 291\text{ kN/m}$, $c = 53\text{ kNs/m}$. Motion compensation applied in x- and y-direction.

CASE 2: 8 MW TOWER

Finally, time domain simulations are carried out to check the response of the 8 MW tower. Installations of the 8 MW tower, or towers with similar dimensions, are expected to be more and more common in the near future. The results for this simulation are obtained using a crane wire length $l_{wr} = 30\text{ m}$ and corresponding optimal values $a = 0.81$, $k = 319\text{ kN/m}$ and $c = 60\text{ kNs/m}$. Again, these parameters represent the condition just before touchdown of the tower.

If one compares the results of the free hanging tower (Fig. 4.23 and Fig. 4.24) with the results of the restrained 8 MW tower (Fig. 4.29 and Fig. 4.30), a similar behavior to that of the restrained 6 MW tower can be observed. However, in contrary to the 6 MW tower the computed most probable maximum values of both the surge and sway response of the tower bottom do fulfill the requirements from Sec. 3.3.

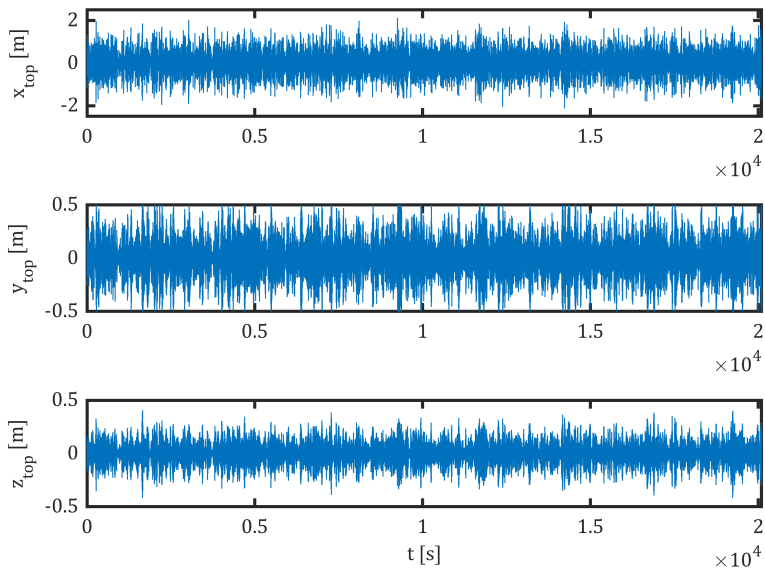


Figure 4.29: Translations of the top of the 8MW tower for $a = 0.81$, $k = 319kN/m$, $c = 60kNs/m$. Motion compensation applied in x- and y-direction.

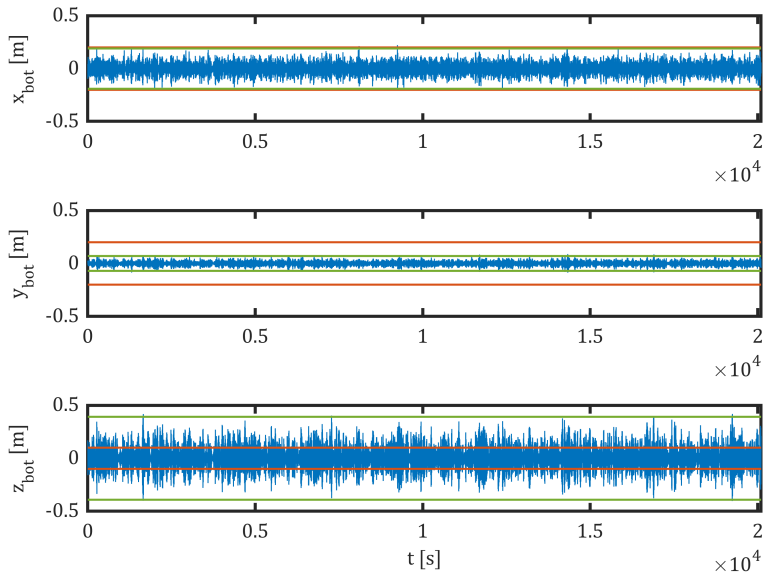


Figure 4.30: Translations of the bottom of the 8MW tower for $a = 0.81$, $k = 319kN/m$, $c = 60kNs/m$. Motion compensation applied in x- and y-direction.

4.5.4. COMPARING THE DIFFERENT SIMULATION METHODS

In Sec. 4.5.2 the standard deviations obtained from the transfer functions derived with the multiple simulation methods have already been compared. The conclusion presented in that section stated that the effect of any non-linearity's on the response of the tower are negligible for the examined sea state. In this section, the results are expanded by adding the standard deviations obtained by the time domain simulations. The results for both the 6 and 8 MW towers are presented in Table 4.5 and Table 4.6. As expected, the standard deviation obtained with the time domain simulation coincide with the earlier results, thereby confirming that linearizing the system gives a good representation of reality.

Table 4.5: Comparing the standard deviations of the response of the 6 MW tower calculated using the different methods.

	SA 6DoF	SA	FD	FD (Mat-lab)	TD
x_{top} [m]	0.50	0.50	0.50	0.51	0.50
x_{bot} [m]	0.11	0.11	0.11	0.11	0.11

Table 4.6: Comparing the standard deviations of the response of the 8 MW tower calculated using the different methods.

	SA 6DoF	SA	FD	FD (Mat-lab)	TD
x_{top} [m]	0.56	0.56	0.56	0.57	0.56
x_{bot} [m]	0.05	0.05	0.05	0.05	0.05

4.5.5. CONCLUSIONS AND DISCUSSION TIME DOMAIN SIMULATIONS

The results of the time domain simulations, presented in the preceding section, are used to analyze the effect of the motion compensation system on the response of the tower. Four important conclusions can be made by analyzing the data.

- The effect of any non-linearity's are negligible for the examined sea state.
- The requirements from Sec. 3.3 are not met and therefore safe installation is not possible using the examined configurations.
- The horizontal displacements of the 8 MW tower can be controlled to within the requirements by applying active motion compensation.
- The vertical motion of the tower exceeds the requirements in all cases and therefore, needs to mitigated.

Although a significant reduction of the bottom motions of the tower can be achieved by application of a motion compensation system, the tower displacements are not reduced to within the requirements, specified in Sec. 3.3, for all cases. To further test and improve

the response of the tower in the crane, one could research the following.

Reconsider the environmental conditions in which safe installation must be possible.

From the optimization process it can be concluded that the response of the system depends on the severity of the environmental conditions. If, in consultation with the client the environmental limit is adjusted downwards, better performances are expected.

Reconsider a different lifting configuration.

From the results of the optimization process it can be concluded that the length of the crane wire has a large effect on the response of the tower. It is expected, the response of the tower can further be mitigated using a different lifting configuration for which the length of the crane wire at the situation just before touchdown is shorter than for the examined cases. However, by doing so, one must make sure a safe distance between the tower and the crane boom is maintained. Changing the lifting configuration can be accomplished in multiple ways:

1. Use a different hoisting arrangement. An offshore crane usually consists of a main hook and one or two auxiliary hooks. One could choose the hoisting arrangement in which the required crane wire length at the moment just before touchdown is the shortest, which will often be the main hook.
2. Reconsider the design of the onboard crane. If one designs the crane boom to be shorter, shorter crane wire lengths can be accomplished.
3. Temporarily shorten the crane wire by locking it to the boom. As a shorter crane boom might not be preferable for all crane operations, one could test the option of temporary locking the crane wire to the crane boom. This is done in practice for lifting of light weight objects, such as wind turbine blades, to control the rotations of the load.

Reconsider a concept without lifting configuration.

By lifting the tower using a crane, the tower has two physical connections with the vessel (via the crane wire and the motion compensation system). Even if the compensation system is able to fully mitigate the vessel motions, the tower top is still connected to the uncompensated crane wire resulting in response motions of the tower. Removing the connection with the uncompensated crane wire, the disturbances at the top of the tower are removed. By doing so, controlling the tower motions is expected to be easier since there is no second factor inducing tower disturbances.

5

CONCLUSION AND RECOMMENDATIONS

The content presented in this thesis covers a study into the different aspects of the installation of an offshore wind turbine tower structure using a HLV. Currently, jack-up vessels are the most common choice for the installation of offshore wind turbines components. For various reasons, however, contractors and engineering firms are searching for alternative methods to install offshore wind turbine components. To study the feasibility of installing offshore wind turbine towers using a HLV, the behavior of a tower with and without motion compensation in the vessel's crane has been examined.

To conclude the study in this report, this final chapter presents the findings of the study and a list of recommendations for future research.

5.1. CONCLUSIONS

To conclude this report, the objectives, introduced in Ch. 2, are discussed in this section. For each objective, the most important findings are presented. The focus of this research has been on controlling the motions of the tower in the crane during installation from a heavy lift vessel, which is in correspondence with the main research objective (as stated below).

Find the most efficient way to control the motions of the wind turbine tower to within safe working limits during installation using a HLV, when taking into account the motions as a result of the environmental conditions.

To achieve the main objective, the following sub-objectives were considered first. An overview of the sub-objectives and the main findings per objective is presented below.

5.1.1. SUB-OBJECTIVES

List the main benefits of installing towers using a HLV.

In Ch. 1 an overview of the different installation methods has been presented. In this chapter floating installation using a heavy lift vessel has been proposed as a good alternative for jack-up installation. The main benefits of floating tower installation with respect to jack-up installation are:

- ability to install both foundations and WTGs
- independency on soil conditions
- no jacking operations required, resulting in shorter installation times

Introduce concepts that allow safe installation of towers using a HLV.

In Ch. 3 a functional design study has been conducted, opting concept solutions that allow the safe installation of offshore wind turbine towers from a floating heavy lift vessel. Project boundaries, requirements and criteria were listed to shape the concept solutions. Two concepts, the Tugger winch concept and the MCPG concept, fulfilled all (initial) requirements.

Create a simplified model to find the optimal installation method.

The model, as presented in Ch. 4, is used to analyze the installation phase just before touchdown of the tower on the TP in the frequency domain. To test the tower response, a generalized model has been made including an active motion compensation system. Using this model, the optimal configuration (position, stiffness and damping) of the motion compensation, in order to minimize the tower response, is determined. The most important conclusions from the model are:

- tower response increases for an increase in crane wire length

In practice, crane drivers often make the crane wire length as long as possible. By doing so, a low frequency response motion is expected for the lifted object. In which case, the crane driver will be able to control the load by steering the crane.

- applying motion compensation does not always result in improvement of the tower response, therefore the configuration of the motion compensation system (position, stiffness and damping) should be chosen with care.

The eigenfrequencies are affected by changing the position (a), stiffness (k) and damping (c) of the motion compensation system. For some configurations, the eigenfrequency of the system coincides with the pitch eigen frequency of the vessel or the peak period of the wave spectrum (Fig. 4.14 and Fig. 4.15). For other configurations the motion compensation system might be positioned at a node of the second eigen mode. In both cases large tower responses are expected.

Create an Orcaflex model to test the tower response using the optimal installation method. To analyze the system in the frequency domain, the vertical motion of the crane tip has been ignored. The effect of this simplification has been tested using Orcaflex. The most important conclusions from the Orcaflex simulations are:

- the effects of ignoring the vertical motion of the crane tip, thereby linearizing the system, are negligible
- the horizontal tower displacements can be mitigated using an active motion compensation system, however safe working limits are not yet met.

5.1.2. MAIN OBJECTIVE

From this study it is possible to conclude that applying active motion compensation can be used to establish a significant reduction of the horizontal displacements of the tower in the crane with respect to a free hanging tower. However, the simulations in this report indicate that the tower motions cannot be controlled to within the motion limits, as set in Sec. 3.3. With that, one can conclude that the most efficient way of controlling the tower motions to within safe working limits using a HLV has not been found.

5.2. RECOMMENDATIONS

Before further analyzing the concepts, the performance of the system must be improved. In Sec. 4.5.5 three proposals have been made to increase the performance of the system. The proposals are shortly discussed here again.

1. Reconsider the environmental conditions in which safe installation must be possible.

The environmental conditions in which the concept should be able to work and the motion limits that must not be exceeded are determined in consultation with, and based on experience of, TWD. However, a more thorough study should be conducted to test those requirements. One could for example study the effect of a bumper/guiding system to guide the tower in position.

2. Reconsider a different lifting configuration.

By choosing a different lifting configuration for which the required length of the crane wire at the moment just before touchdown is smaller, the horizontal tower response is

expected to be smaller. This effect will result in a better performance of the system.

3. Reconsider a concept without lifting configuration.

The tower has two physical connections to the HLV when lifted with a crane. The first connection, between tower and HLV, will be via the uncompensated crane wire and the second via the motion compensation system. Even if the motion compensation system will maintain its exact position throughout the operation, motions are induced on the tower through the connection with the crane tip. If one removes this connection, compensating the tower motions is expected to become easier. However, a concept like this will require a lot of innovation and an onboard crane will often be required for activities like on- and offloading.

The simulations performed in this report are a simplification of reality and therefore, if one chooses to further analyze one of the concepts, the recommendations (4,5 and 6) presented below should be followed.

4. Study the effect of different wave headings on the response of the tower.

In reality waves will not travel strictly in one direction. Therefore, the assumption that all waves will encounter under an angle of 180 degrees does not resemble reality. Furthermore, the captain will not always be able to position the vessel in such a way that it is subjected to head waves. Therefore, the effect of multiple incoming wave directions should be examined to obtain more reliable results. For different wave headings, the crane tip sway will become important and a circular motion of the tower is expected.

5. Examine the effect of wind and second order vessel motions on the response of the tower.

For a free hanging object, the wind and second order vessel motions will result in a low frequency response motion of the lifted object. Such low frequent motions can, in reality, often be mitigated by the crane driver. The concepts proposed in this research, however, retain the tower at a point along the height, which can result in unexpected behavior of the tower. Therefore, it would be interesting to check the effect of wind and second order vessel motions in combination with the concepts.

6. Study the effect of mitigating the heave motions of the tower.

To ensure safe installation, the vertical displacements of the tower should not exceed the limits specified in Sec. 3.3. Without compensation in vertical direction, the vertical motion of the tower does not fulfill this requirement and therefore safe installation is not possible.

BIBLIOGRAPHY

- BloombergNEF. 2h 2017 offshore wind market outlook. Technical report, BloombergNEF, 2017.
- DNV. *DNV-RP-H103 Modelling and analysis of marine operations*. Det Norske Veritas, April 2011.
- G. González. *A pendulum with a moving support*. Louisiana State University, 2006.
- GWEC. *Global Wind 2017 Report*, chapter A Snapshot of Top Wind Markets in 2017: Offshore Wind. Global Wind Energy Council, 2018.
- WindEurope Business Intelligence. Offshore wind in europe. Technical report, WindEurope, 2018.
- J.M.J. Journée, W.W. Massie, and R.H.M. Huijsmans. *Offshore Hydromechanics*. Delft University of Technology, 3 edition, 2015.
- D.J. Rixen. *Engineering Dynamics*. TU Delft, 2006.
- K.J. Åström and R.M. Murray. *Feedback Systems; An introduction for scientists and engineers*. Princeton University Press, v2.11b edition, 2008.
- A. van Boeijen and J. Daalhuizen. *Delft Design Guide*. TU Delft, 2010.

A

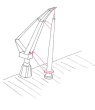
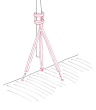
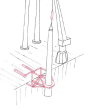

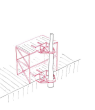
CONCEPT EVALUATION

The concepts, as proposed in Ch. 3, provided a guideframe throughout this thesis on which certain design considerations are based. As the concepts were developed during the first months of the research, without clear knowledge about the dynamics of the system, the concept designs differ in size and working principle. Using a multi-criteria analysis in Sec. 3.5.1 a first selection between the concepts has been made based on a list of design criteria. Taking the results of the motion analysis in consideration, one can analyze the viability of the selected concepts in more detail. To test the feasibility of the concepts discussed in this thesis, the system has been modelled using Matlab and Orcaflex. The results of the simulations can be used to reconsider the concepts.

A.1. CONCEPT RE-EVALUATION

In Ch. 3 a first selection between the different concepts has been made by application of a multi-criteria analysis. The concepts have been tested against a list of criteria, which were introduced to compare the designs regarding its complexity, costs and performance. The engineering models of product design (Sec. 3.1), on which TWD's functional design method is based, state that the design process is an iterative process during which constant re-evaluation of the concepts is required. In this thesis, the response of a tower in a crane, with and without application of a motion compensation system, has been studied into more detail. The results of this study, although not exactly representing the concepts, can be used to re-evaluate some of the criteria presented in Sec. 3.5.1. The initial multi-criteria analysis, as discussed in Sec. 3.5.1, is presented in Table A.1, where the orange colored planes indicate the criteria and concepts that cannot be used for re-evaluation of the concepts.

Table A.1: Multi-criteria analysis of the different concepts.

MCA Ranked from 1 to 5	Weight factor	 Concept 1	 Concept 2	 Concept 3	 Concept 4	 Concept 5
Design complexity	2	++	±	±	-	-
Operational costs						
Workability	4	+	+	+	++	+
Number of trips	2	+	+	±	+	-
Power consumption	3	++	++	±	-	-
Maintenance required	1	++	-	-	-	-
Construction costs						
Structural costs	2	\$	\$\$	\$\$\$	\$\$\$\$\$	\$\$\$\$
Manufacturability	4	++	+	±	-	-
Overall project duration						
Installation efficiency	4	±	+	±	+	-
Operational cycle time	4	+	+	+	++	-
Ability to install						
Various tower dimensions	5	++	++	++	++	+
Tower sections	1	+	-	-	++	++
Tower and nacelle	5	-	+	-	-	-
Robustness	4	-	+	-	+	-
Vessel independent	2	+	+	++	-	-
Lifetime/durability	3	-	+	+	+	+
Weighed total		168	186	146	141	103

The ratings in Table A.1 can be assigned a value ranging from 1 to 5 by applying the scaling factors presented in Table A.2. The weighed total is the sum of the individual ratings.

Table A.2: Scaling factors used to score the concepts.

General	-	-	±	+	++
Costs	\$\$\$\$	\$\$\$	\$\$\$	\$\$	\$
Weight	1	2	3	4	5

A.1.1. OPTIMAL CONFIGURATIONS

In this section, the simulation results will be used to re-evaluate the Tugger winch and MCPG concepts. The optimal parameters (a, k and c) of the motion compensation system, found in Ch. 4, can be used to make a first assessment of the design complexity and structural considerations.

In Sec. 4.4 an optimization strategy has been proposed to determine the optimal configuration of the motion compensation system for the 6 and 8 MW towers at the moment just before touchdown of the tower on the transition piece. The results of the optimization process show that the optimal configuration of the motion compensation system, in order to minimize the tower response, depends on the dimensions of the tower, the length of the crane wire and the environmental conditions.

To determine the optimal configurations, environmental conditions are simulated using a JONSWAP spectrum with a significant wave height $H_s = 2.5m$ and peak period $T_p = 9s$. For these conditions, the optimum motion compensation parameters are:

$$6MW: a = 0.69, k = 291 \text{ kN/m}, c = 53 \text{ kNs/m}$$

$$8MW: a = 0.81, k = 319 \text{ kN/m}, c = 60 \text{ kNs/m}$$

Up till now, representations of the vessel and tower have been used for clarifying purposes only. Although throughout the report a representation of reality is pursued, the scale in the figures might be a bit off. To indicate the effect of the optimal configurations in reality, a schematic representation of the vessel, tower and optimal compensation heights is presented in Fig. A.1. The ratios in this figure do resemble a real situation.

A first thing to note is the difference in height between the vessel's main deck level (6 m above the still water level (SWL)) and the landing platform of the transition piece (25 m above SWL). In the figure, two horizontal lines are drawn representing the optimal compensation heights at respectively 69% and 81% of the tower length. From the figure it can be noted that, to minimize the tower response, the compensation system should be positioned at either 57 m above SWL for the 6 MW tower or 47 m above SWL for the 8 MW tower.

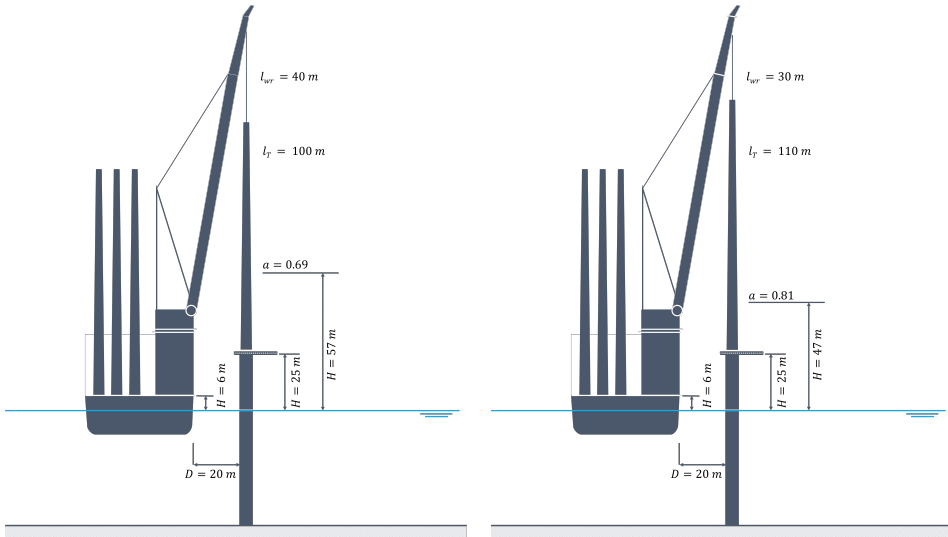


Figure A.1: Optimal configuration for the 6 MW tower [l], Optimal configuration for the 8 MW tower [r]

The information in this figure, together with the results of the motion analysis, can be used to re-evaluate the concepts.

CONCEPT 1: TUGGER WINCHES

The first concept to be re-evaluated, looking at the results of the optimization study, is the tugger winch concept. The performance of the motion compensation system, as discussed in Sec. 4.5.5, does not yet fulfill the requirements. At the end of this chapter proposals are made to improve the performance. The concept is evaluated using the remaining criteria from Table A.1 of which the results are presented in Table A.3.

Table A.3: Initial and updated ratings of the Tugger winch concept.

	Initial	Eval 1
Design complexity	++	+
Workability	+	±
Structural costs	\$	\$\$
Manufacturability	++	+
Various tower dimensions	++	+
Tower sections	+	±
Robustness	-	-
Vessel independent	+	+

The results from the study into the effect of lifting and lowering on the response of the tower (Sec. 4.4) indicate that the optimal position of the compensating system along the height of the tower changes during lowering and lifting of the tower. By changing the

position of the winches along the length of the crane boom one can, in theory, maintain the position in which the force transmission is optimal. However, since the tugger lines are connected to the tower it will be harder to change the position of the tugger line connection during the installation process. To accomplish this, the complexity of the design will increase slightly and with that the structural costs are likely to increase as well. Due to the increasing complexity of the design, it is expected the construction of the design will take a bigger effort and therefore the manufacturability is assigned a lower value.

A major benefit of this concept is its ability to be applied at big heights, without the need for a very large structure (Fig. A.2). Therefore, no further increase of the structural costs is required.

From the analysis into the effect of lifting and lowering on the response of the tower (see Sec. 4.4), one can conclude that an increase in crane wire length results in a bigger response of the tower. Therefore, installing the tower in smaller sections is expected to result in larger tower motions. However, by dividing the tower in sections the mass and inertia of the lifted objects change and therefore the results of the analysis, conducted in Sec. 4.4, should be re-examined for smaller tower lengths to support this theory.

The robustness of the design is not expected to change much, since it still consists of winches and a connection of cables to the tower. Furthermore, the system can, in theory, still be applied at different vessels and therefore the vessel dependency is not expected to change.

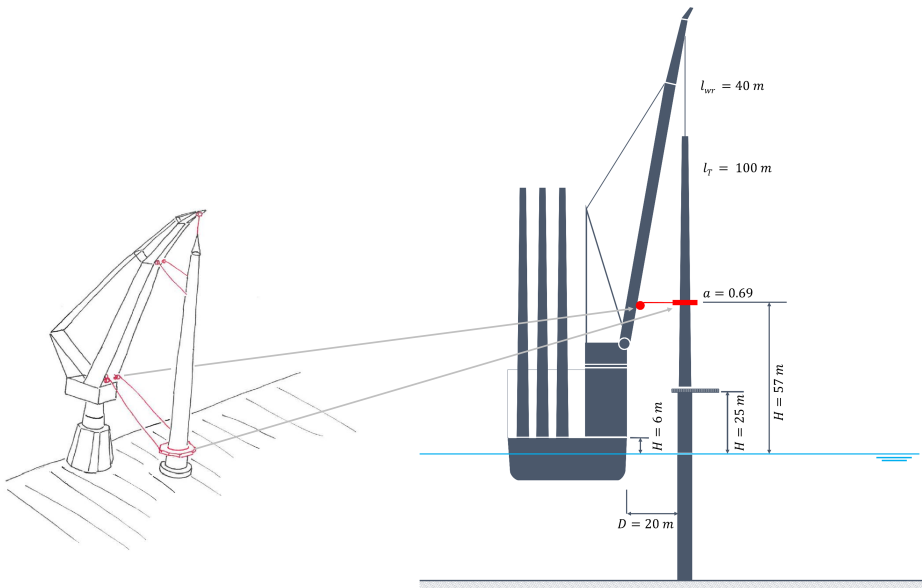


Figure A.2: Schematical representation of the Tugger winch concept

CONCEPT 3: MCPG

The second concept to be re-evaluated is the MCPG concept. The concept's performance, as discussed in Sec. 4.5.5, does not yet fulfill the requirements. At the end of this chapter proposals are made to improve the performance. The concept has been evaluated again using the remaining criteria from Table A.1 of which the results are presented in Table A.4.

Table A.4: Initial and updated ratings of the MCPG concept.

	Initial	Eval 1
Design complexity	±	±
Workability	+	±
Structural costs	\$\$\$	\$\$\$\$
Manufacturability	±	-
Various tower dimensions	++	++
Tower sections	-	-
Robustness	-	-
Vessel independent	++	++

The results of the study into the effect of lifting and lowering of the tower (Fig. 4.13) show that the optimal position of the compensation system along the height of the tower changes with approximately the same rate as the length of the crane wire (for $T_p = 9s$). Therefore, it would, in theory, be possible to choose the initial position of tower and compensating system in such a way that the optimal position of the compensating system can be maintained during lifting and lowering. However, considering the results of the optimization process, one can conclude that a very large structure (pedestal) will be required on board to assist the concept in applying compensation at the optimal height (Fig. A.3). Installation of such a structure on deck increases the structural costs of the design. The design of a pedestal is expected not to influence the overall design complexity as the motion compensation system is much more complex. The weight of the structural costs and the manufacturability, however, are expected to increase due to the costs of the additional material and construction time required for the pedestal.

As the concept will be positioned at a fixed height with respect to the vessel's main deck, installing a tower in different sections is not possible. The robustness of the concept itself will not change by positioning it at a different height and the independency on the vessel, provided there is enough space on the vessel, will also not change.

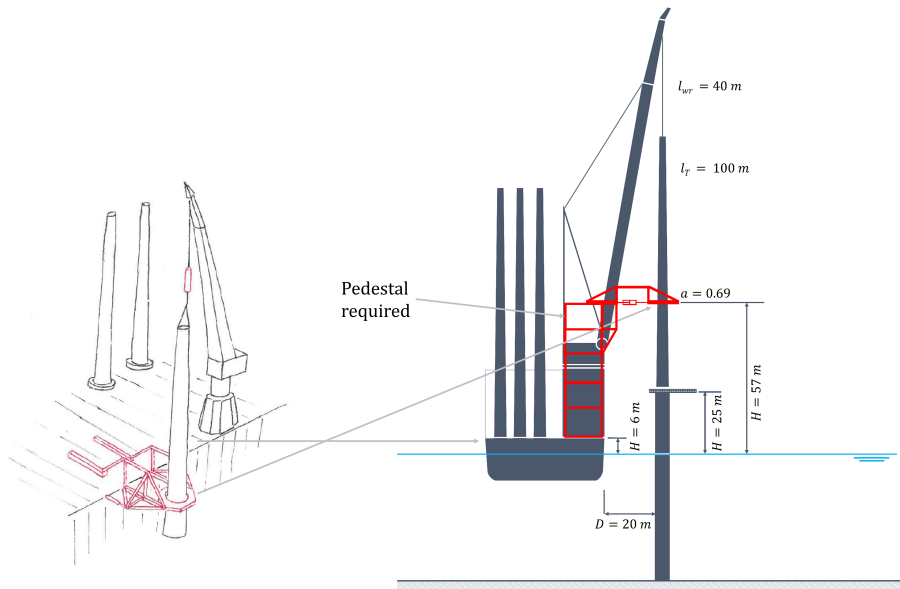


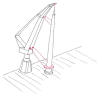
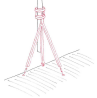
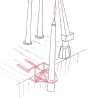


Figure A.3: Schematical representation of the MCPG concept

A.2. CONCLUSIONS

The results of re-evaluating the concepts against the criteria from Ch. 3 are summarized here again. The updated concept ratings are used to update the multi-criteria analysis of Sec. 3.5.1 and presented in Table A.5. New overall scores for the Tugger winch and MCPG concept are obtained and can be used to update the design considerations.

The updated ratings, see Table A.5, show that after the evaluation step the Tugger winch concept is still preferred above the MCPG concept. As the workability of both concepts is assumed similar, the difference is mainly caused by the costs and complexity of the design. The Tugger winch concept is expected to be more cost efficient and scores better for it.

Table A.5: Multi-criteria analysis of the different concepts.

MCA						
	Weight factor	Concept 1	Concept 2	Concept 3	Concept 4	Concept 5
Ranked from 1 to 5						
Design complexity	2	+	±	±	-	-
Operational costs						
Workability	4	±	+	±	++	+
Number of trips	2	+	+	±	+	-
Power consumption	3	++	++	±	-	-
Maintenance required	1	++	-	-	-	-
Construction costs						
Structural costs	2	\$\$	\$\$	\$\$\$\$	\$\$\$\$\$	\$\$\$\$
Manufacturability	4	+	+	-	-	-
Overall project duration						
Installation efficiency	4	±	+	±	+	-
Operational cycle time	4	+	+	+	++	-
Ability to install						
Various tower dimensions	5	++	++	++	++	+
Tower sections	1	±	-	-	++	++
Tower and nacelle	5	-	+	-	-	-
Robustness	4	-	+	-	+	-
Vessel independent	2	+	+	++	-	-
Lifetime/durability	3	-	+	+	+	+
	Weighed total	155	186	136	141	103

To justify a decision to continue with one of the concepts, more research into the concepts is required. The first step must be to test the design against the remaining criteria.

The remaining criteria focus mainly on the installation vessel outfitted with the concept, thereby considering the number of trips required to install a certain number of turbines, the installation efficiency, the operational cycle time and the expected lifetime of the concept. Due to a lack of time and divergent scope, the influence of these criteria has not been examined. To be able to compare the concepts against each other, more information is required about the performance of the concepts and the time required to install a tower using the concept.